gene dosage-dependent effects of Ptpn11 mutation. *Nat Med* 2004; **10**: 849–857.
47 Donovan S, See W, Bonifas J, Stokoe D, Shannon KM. Hyperactivation of protein kinase B and ERK have discrete effects on survival, proliferation, and cytokine expression in Nf1-deficient myeloid cells. *Cancer Cell* 2002; **2**: 507–514.
48 Yokomizo T, Ogawa M, Osato M, Kanno T, Yoshida H, Fujimoto T *et al.* Requirement of Runx1/AML1/PEBP2alphaB for the generation of haematopoietic cells from endothelial cells. *Genes Cells* 2001; **6**: 13–23.
49 Care RS, Valk PJ, Goodeve AC, Abu-Duhier FM, Geertsma-Kleinekoort WM, Wilson GA *et al.* Incidence and prognosis of c-KIT and FLT3 mutations in core binding factor (CBF) acute myeloid leukaemias. *Br J Haematol* 2003; **121**: 775–777.
50 Wang YY, Zhou GB, Yin T, Chen B, Shi JY, Liang WX *et al.* AML1-ETO and C-KIT mutation/overexpression in t(8;21) leukemia: implication in stepwise leukemogenesis and response to Gleevec. *Proc Natl Acad Sci USA* 2005; **102**: 1104–1109.
51 Kohl TM, Schnittger S, Ellwart JW, Hiddemann W, Spiekermann K. KIT exon 8 mutations associated with core binding factor (CBF) – acute myeloid leukemia (AML) cause hyperactivation of the receptor in response to stem cell factor. *Blood* 2004; **105**: 3319–3321.
52 Yang G, Khalaf W, van de Locht L, Jansen JH, Gao M, Thompson MA *et al.* Transcriptional Repression of the neurofibromatosis-1 tumor suppressor by the t(8;21) fusion protein. *Mol Cell Biol* 2005; **25**: 5869–5879.
53 Johnson EJ, Scherer SW, Osborne L, Tsui LC, Oscier D, Mould S *et al.* Molecular definition of a narrow interval at 7q22*1 associated with myelodysplasia. *Blood* 1996; **87**: 3579–3586.
54 Grisendi S, Bernardi R, Rossi M, Cheng K, Khandker L, Manova K *et al.* Role of nucleophosmin in embryonic development and tumorigenesis. *Nature* 2005; **437**: 147–153.

Supplementary Information accompanies the paper on the Leukemia website (http://www.nature.com/leu)

Molecular Cell
Article

Cytokines Direct the Regulation of Bim mRNA Stability by Heat-Shock Cognate Protein 70

Hirotaka Matsui,[1] Hiroya Asou,[1] and Toshiya Inaba[1,*]
[1] Department of Molecular Oncology and Leukemia Program Project, Research Institute for Radiation Biology and Medicine, Hiroshima University, Hiroshima 734-8553, Japan
*Correspondence: tinaba@hiroshima-u.ac.jp
DOI 10.1016/j.molcel.2006.12.007

SUMMARY

Previous gene-targeting studies indicated that Bim, a BH3-only death activator, regulates total blood cell number. Cytokines contribute to this process by negatively regulating steady-state levels of Bim mRNA. Here we present a molecular mechanism for cytokine-mediated posttranscriptional regulation of Bim mRNA by heat-shock cognate protein 70 (Hsc70), which binds to AU-rich elements (AREs) in the 3′-untranslated region of specific mRNAs and enhances their stability. The RNA binding potential of Hsc70 is regulated by cochaperones including Bag-4 (also SODD), CHIP, Hip, and Hsp40. Cytokines regulate the expression or function of these cochaperones by activating Ras pathways. Thus, exposure of cells to cytokines ultimately leads to destabilization of Bim mRNA and promotion of cell survival. This unanticipated role of a chaperone/cochaperone complex in mRNA stability appears to be critical for hematopoiesis and leukemogenesis.

INTRODUCTION

Cytokines promote cell survival of hematopoietic progenitors by negative regulation of Bim (O'Connor et al., 1998; Hsu et al., 1998), a BH3-only cell death activator in the Bcl-2 superfamily (reviewed in Inaba [2004]). Neurotrophic factors promote the survival of neuronal cells, also by negative regulation of Bim (reviewed in Freeman et al. [2004]). Bim-deficient mice, which manifest both hyperplasia of hematopoietic progenitors and increased white blood cell count (Bouillet et al., 1999), support Bim's role in hematopoiesis. In addition, T cell development is perturbed, and older knockout mice accumulate plasma cells and succumb to autoimmune kidney disease. Cytokines also control the activity of $p27^{KIP1}$ (Toyoshima and Hunter, 1994). Disruption of the murine p27 gene results in hyperplasia of all organs, including hematopoietic progenitors in the spleen and T cells in the thymus (Fero et al., 1996). Thus, cytokine regulation of Bim and p27 is critical for cell-number homeostasis, especially in the hematopoietic and immune systems.

The molecular mechanisms by which cytokines negatively regulate Bim function differ between cell types. At least three different mechanisms have been reported (reviewed in Inaba [2004]). First, steady-state levels of Bim mRNA decrease in the murine hematopoietic progenitor cell lines Baf-3 and FL5.12 in response to IL-3-mediated activation of Ras pathways (Shinjyo et al., 2001; Dijkers et al., 2000a). Nerve growth factor (NGF) functions similarly as a negative regulator of Bim in primary cultures of rat sympathetic neurons and PC-12 cells (reviewed in Freeman et al. [2004]). Second, serum- or cytokine-dependent phosphorylation of Bim enhances its ubiquitination, which is known to regulate the proteasome-dependent degradation of Bim in serum-deprived fibroblasts and M-CSF-dependent osteoclasts (Ley et al., 2003; Akiyama et al., 2003; Luciano et al., 2003). Third, IL-3 affects the subcellular localization of Bim in murine FDC-P1 cells (Puthalakath et al., 1999), in which IL-3 promotes Bim binding to dynein motor complexes on microtubules. Upon withdrawal of IL-3, Bim dissociates from microtubules and then binds to and inhibits antiapoptotic Bcl-2 protein function.

The diversity of these regulatory mechanisms suggests that regulation of Bim function is multifaceted, allowing flexibility in Bim's response to different signals or in different cell types (Yamaguchi et al., 2003). Observations in our laboratory demonstrate that hematopoietic homeostasis is sensitive to changes in steady-state Bim mRNA levels, in that Bim mRNA levels increase in bone marrow-derived $Sca\text{-}1^{+}c\text{-}Kit^{+}Lin^{-}$ cells that are deprived of stem cell factor (SCF) and thrombopoietin (TPO) (Kuribara et al., 2004). In addition, recent studies indicate that cytokines also regulate steady-state levels of p27 mRNA (Dijkers et al., 2000b; Parada et al., 2001; Stahl et al., 2002), although, prior to these reports, regulation of p27 activity was thought to occur predominantly via cyclin E-cdk2-mediated phosphorylation, which targets p27 for proteasome-dependent degradation. These results suggest that cytokine deprivation can decrease cell number in the body by promoting increases in Bim and p27 mRNA levels.

NGF-mediated regulation of Bim in PC12 cells depends on sequence-specific DNA binding sites for FOXO3a (also

FKHR-L1), located in the Bim enhancer (Gilley et al., 2003). p27 gene transcription in Baf-3 cells has also been reported to be regulated by FOXO3a (Dijkers et al., 2000b). Since FOXO3a is inactivated by Ras-mediated phosphorylation events (reviewed in Birkenkamp and Coffer [2003]), we initially hypothesized that FOXO3a regulated the cytokine-dependent transcription of Bim in hematopoietic cells. However, experiments in Baf-3 cells demonstrated no IL-3-dependent *cis*-acting regulatory elements in Bim (Matsui et al., 2005). Furthermore, FOXO3a binding sites within Bim (which function as NGF-dependent enhancers in PC12 cells) did not affect Bim transcription efficiency in Baf-3 cells, and de novo transcription of Bim in Baf-3 cells was similar in the presence or absence of IL-3. These data led to the alternative hypothesis that IL-3-dependent decreases in Bim mRNA levels occur posttranscriptionally.

Here, we report that cytokines regulate Bim mRNA stability in Baf-3 cells. Binding of heat-shock cognate protein 70 (Hsc70), which stabilizes Bim mRNA, is regulated by the cytokine-dependent association of cochaperones with Hsc70. We suggest that this mechanism plays a critical role in the regulation of hematopoietic cell number in the body.

RESULTS

Destabilization of Bim mRNA by IL-3 in Baf-3 Cells

The 3′UTR of human Bim mRNA is long (4.2 kb) relative to the coding region (0.6 kb) (Figure 1A). The 3′UTR contains a number of AUUUA pentamer repeats, which are *cis*-acting sequences within AU-rich sequence elements (AREs) that are critical to the regulation of mRNA stability. In a comparison between the eight pentamers in human mRNA and six in mouse mRNA, four are conserved. Although the overall sequence homology is low between human and mouse Bim 3′UTRs, there is 76% conservation within a 1 kb region that includes three AUUUA pentamers.

To assess the role of the Bim 3′UTR on mRNA stability, IL-3-dependent Baf-3 cells were transfected with Tet-regulated plasmids expressing full-length β-globin mRNA (control) or an mRNA hybrid of β-globin coding sequence terminated by the Bim 3′UTR. Expression was induced for 3 hr and then shut off. mRNA decay was measured by using ribonuclease protection assay (RPA) and real-time quantitative RT-PCR (qRT-PCR). As previously demonstrated (Xu et al., 1998), full-length β-globin mRNA expressed in Baf-3 cells was stable in the presence or absence of IL-3 (Figures 1B and 1C). In contrast, the stability of the β-globin/Bim hybrid mRNA was reduced significantly in the presence of IL-3.

The half-lives of Bim, p27, and c-*fos* mRNAs synthesized and radiolabeled in vitro were measured in Baf-3-cell cytosol (S100) extracts. The half-life of a 1 kb Bim mRNA encompassing the conserved region between human and mouse 3′UTRs was less than 10 min in extracts from IL-3-treated Baf-3 cells (Figures 1D and 1E) but increased significantly to ~30 min in extracts prepared from cells without IL-3. The half-life of p27 3′UTR mRNA increased similarly in IL-3-starved cell extracts. IL-3-dependent message destabilization in Baf-3 extracts was not universal, since the half-lives of c-*fos* mRNA (<10 min) and GAPDH mRNA (>30 min) remained constant in the presence or absence of IL-3. Moreover, the 30 min half-life of Bim mRNA in lysates from FDC-P1 cells (another IL-3-dependent cell line in which Bim expression is not affected by IL-3) did not vary in the presence or absence of IL-3.

mRNA decay generally initiates with poly(A) tail deadenylation followed by degradation of internal sequences. To observe shortening of the poly(A) tail, we repeated the in vitro RNA decay assay using short mRNAs (~60 bases) containing native AREs and a 100 base poly(A) tail. With or without IL-3, deadenylation of GAPDH control mRNA was detected at 20 min, similar to Bim and p27 mRNAs in cytosol preparations from IL-3-starved Baf-3 cells (Figure 1F). In contrast, deadenylation of Bim and p27 mRNAs initiated within 5 min and progressed rapidly in extracts from IL-3 treated Baf-3 cells. When 5′-capped Bim mRNA without a poly(A) tail was mixed with Baf-3 cell extracts, both the 1 kb conserved region and the short ARE in the 3′ UTR degraded more rapidly in the presence of IL-3 (Figure 1G). These data demonstrate that IL-3 destabilization of mRNAs in Baf-3 cells is gene and cell type specific and occurs by stimulation of mRNA deadenylation and degradation.

Hsc70 Binds to Bim mRNA in an IL-3-Dependent Manner

To identify RNA binding proteins that may function as IL-3-dependent stabilizing or destabilizing factors, RNA-affinity chromatography was used to enrich for cytosolic proteins that bind to Bim's 3′UTR. When cytosolic extracts of Baf-3 or FL5.12 cells were exposed to columns coupled with the 3′UTR of Bim or p27 mRNA, the bound fractions resolved with similar patterns in SDS-polyacrylamide gels (Figure 2A). In particular, the intensity of one band (~75 kDa) was greater in IL-3-starved Baf-3 or FL5.12 cells relative to cells cultured with IL-3. In contrast, the signal from the 75 kDa band was weak and did not vary in the presence or absence of IL-3 when eluted from GAPDH (containing no ARE) or c-*fos* 3′UTR mRNA columns. The pattern of FDC-P1 extract proteins bound to Bim mRNA showed significantly less 75 kDa signal.

Polypeptide bands at the position of 75 kDa were excised from the gel and analyzed by using a MALDI-TOF/TOF mass spectrometer. In peptide mass fingerprinting, the molecular weights of nine peaks matched mouse Hsc70 (Figure 2B), and mass spectrometric sequencing of these peaks also matched Hsc70 (Figure 2C). Proteins bound to the Bim 3′UTR column showed a 6-fold increase in reactivity to Hsc70-specific antibody when isolated from IL-3 starved Baf-3 cells relative to cells grown with IL-3 (Figure 2D), whereas the Hsc70 signal was weak in Bim 3′UTR binding proteins from FDC-P1 cells both in the presence and absence of IL-3. No Hsp70 (closely

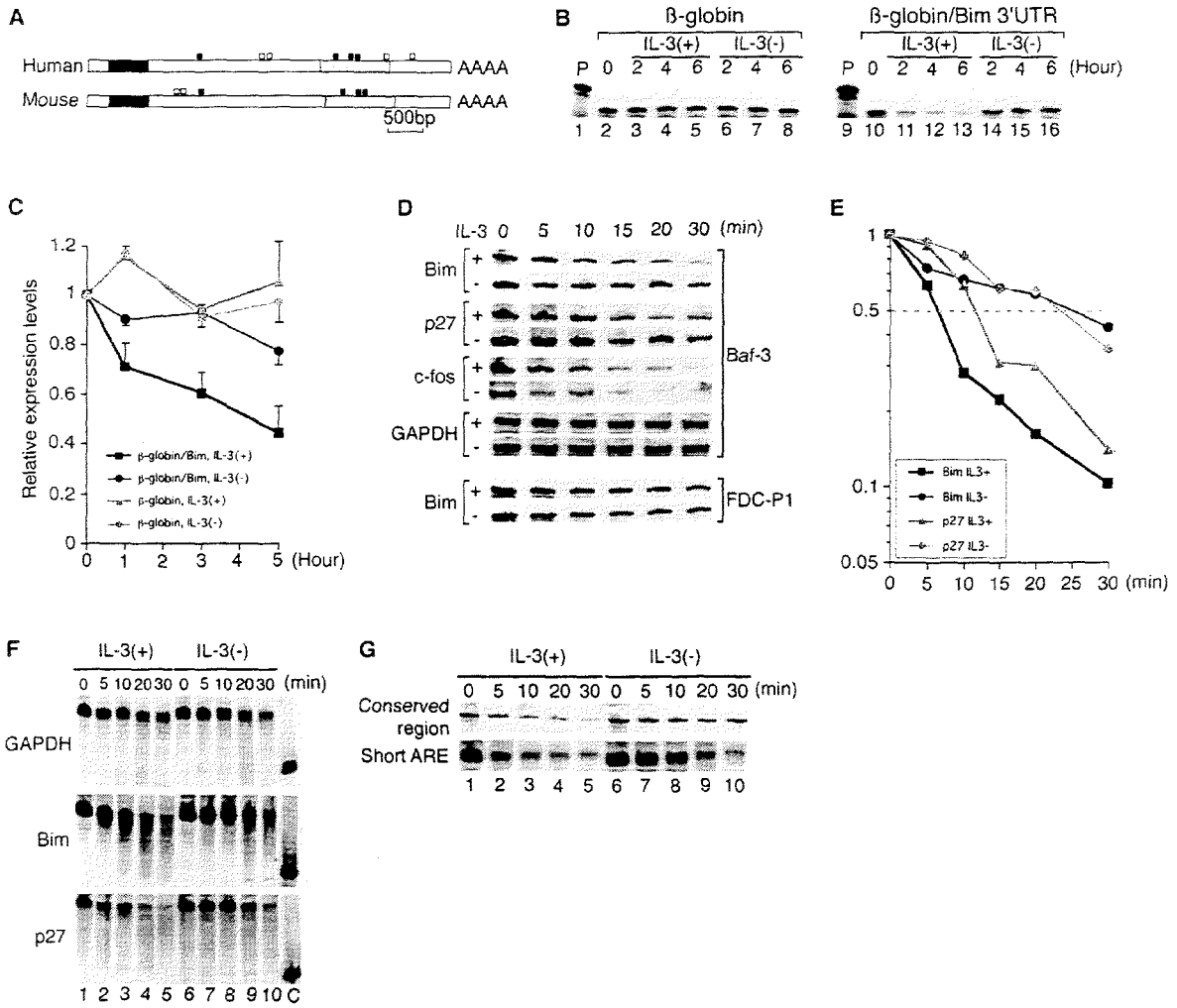

Figure 1. Stability of Bim mRNA

(A) A schematic representation of human and mouse Bim mRNAs. Black bars represent the coding regions, open bars untranslated regions, and gray bars regions of strong homology between human and mouse. Black squares above bars indicate AUUUA pentamers conserved between the human and mouse 3'UTRs; open squares are those present in either human or mouse.

(B and C) Stability of a β-globin/Bim 3'UTR fusion mRNA and β-globin mRNA (control) transiently expressed in Baf-3 cells cultured in the presence or absence of IL-3 and measured using RPA (B) or qRT-PCR (C). The mean and SD of three independent experiments are shown.

(D–G) RNA-stability assays in vitro. Cytosol preparations from Baf-3 or FDC-P1 cells (D, indicated at right) cultured in the presence or absence of IL-3 were incubated for indicated periods with radiolabeled and capped mRNAs (genes marked at left) with (D–F) or without (G) a poly(A) tail of 100 residues. Values for each band were measured and plotted as percent relative to starting point levels (E).

related to Hsc70) was detected in the Bim 3'UTR-bound fraction of Baf-3 cells grown in the presence or absence of IL-3.

Hsc70 and Hsp70 have been shown to bind to AREs (Henics et al., 1999; Wilson et al., 2001; Duttagupta et al., 2003), and its binding is enhanced by Hsp40 (Zimmer et al., 2001). Binding of Hsc70 to Bim mRNA and the effect of recombinant Hsp40 (DjB1) protein was tested in vitro with a Bim 3'UTR probe containing two conserved AUUUA pentamers. Although the probe was not shifted above background in the presence of Hsc70 or Hsp40 alone, an equimolar mixture of Hsc70, Hsp40, and a co-chaperone, Hip (Hohfeld et al., 1995; we discuss later in detail) retarded the mobility of the RNA (Figure 2E). In the presence of Hsc70 or Hsp40 antibodies, the mobility of this complex was retarded further, suggesting that two proteins coassociate with Bim mRNA.

To test whether Hsc70 binds to RNA directly, mixtures of recombinant Hsc70, Hsp40, and Hip with radiolabeled AREs of Bim, GAPDH, or c-fos were UV crosslinked and resolved by SDS-PAGE. A single protein band of ~75 kDa was observed with a Bim mRNA probe, but not with GAPDH or c-fos probes (Figure 2F, lanes 1–3). In experiments using extracts from Baf-3 cells cultured with or

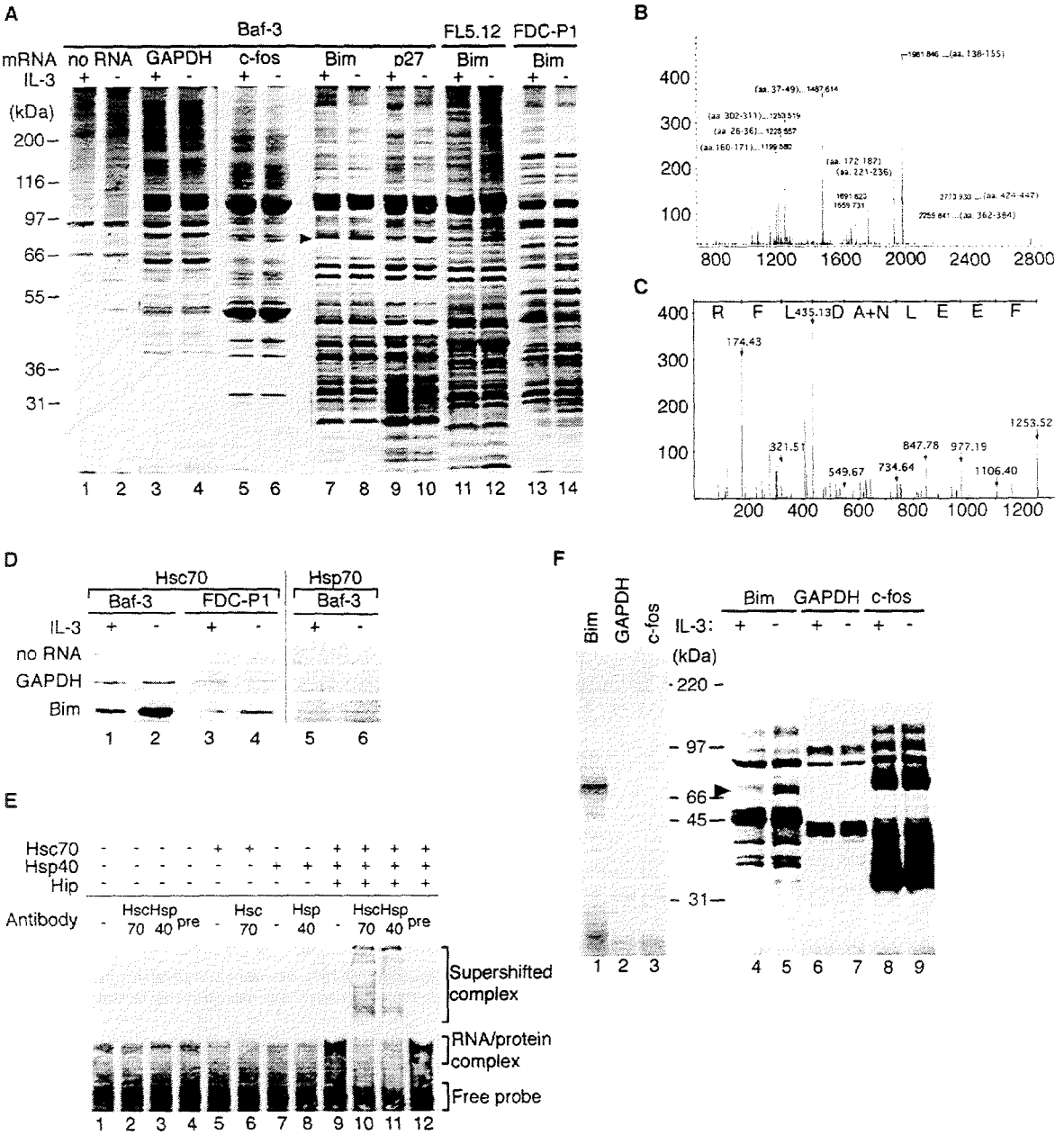

Figure 2. Hsc70 Binds to Bim mRNA

(A) RNA-affinity chromatography to enrich for proteins (in the cell types indicated above) that bind to the 3′UTRs of GAPDH, c-*fos*, Bim, or p27 mRNAs. Proteins were visualized by silver staining. An arrowhead indicates bands analyzed by MALDI-TOF/TOF.

(B) A representative result of peptide mass fingerprinting from MALDI-TOF analysis. The molecular weight of each peak and the corresponding amino acid residues of Hsc70 are shown.

(C) An example of protein sequencing using MALDI-TOF/TOF analysis. The MS/MS spectrum was recorded from the fragmentation of an ion at 1253.519. The interpretation of this spectrum gave the putative sequence FEEL(A+N)DLFR, where (A+N) denotes either AN or NA. This sequence matched aa 302–311 (FEELNADLFR) in mouse Hsc70.

(D) Hsc70- or Hsp70-specific antibody was used in immunoblots of fractions of Baf-3 and FDCP-1 cell extracts that bound to beads with no RNA, the 3′UTR of GAPDH or Bim mRNA.

(E) RNA gel retardation assay. A radiolabeled Bim mRNA probe was mixed with recombinant proteins as indicated above. Anti-Hsc70, anti-Hsp40, or preimmune serum was present as indicated.

(F) UV-crosslinking assay. Mixture of recombinant Hsc70, Hsp40, and Hip (lanes 1–3) or Baf-3 cell lysates cultured in the presence or absence of IL-3 (lanes 4–9) was incubated with radiolabeled Bim, GAPDH, or c-*fos* mRNA. An arrowhead indicates a band enhanced by IL-3 starvation.

without IL-3 (lanes 4–9), numerous protein bands were detected, including one at 75 kDa that was relatively more abundant in cells grown in the absence of IL-3 (arrowhead), while other crosslinked complexes were similar in intensity in cells grown with or without IL-3. When the same extracts were crosslinked with GAPDH or c-*fos* 3′UTR mRNAs, banding patterns differed substantially and showed little 75 kDa complex. These results indicated that Hsc70 interacts directly with Bim mRNA.

Hsc70 Stabilizes Bim mRNA

We established Baf-3 cells expressing Hsc70 at low levels using short hairpin RNA (shRNA)-expression plasmid vectors, piGENE-mU6-Hsc70#5 and #6, each of which targets a different sequence in Hsc70 mRNA. In two representative clones, #5-7 and #6-6 (Figure 3A), transiently expressed β-globin/Bim hybrid mRNA degraded rapidly in the presence or absence of IL-3, whereas steady-state levels of full-length β-globin mRNA were stable (Figure 3B). In in vitro mRNA decay assay, rapid deadenylation and degradation of Bim mRNA in extracts from clones #5-7 and #6-6 was observed regardless of IL-3 presence (Figure 3C).

IL-3 starvation increases steady-state levels of Bim mRNA in parent Baf-3 cells (Shinjyo et al., 2001) (Figure 3D and 3E). Consequently, upon removal of IL-3, steady-state levels of BimEL, BimL, and BimS proteins (encoded by alternatively spliced mRNAs) increase steadily (Figure 3F), and massive cell death initiates approximately 12 hr after IL-3 removal (Figure 3G). Relative to parent Baf-3 cells, IL-3 starvation weakly increased Bim mRNA levels in #5-7 and #6-6 cells (Figures 3D and 3E), yielding only marginal increases in Bim proteins (Figure 3F) and delaying apoptosis (Figure 3G). These data suggest that increases in the steady-state level of Bim mRNA are due primarily to mRNA stabilization and accumulation, which occur by Hsc70 stabilization of mRNAs in response to cytokine starvation.

Cochaperones Regulate the RNA Binding Potential of Hsc70

Since IL-3 starvation had no effect on the steady-state levels of Hsc70 protein in Baf-3 cells (Figure 4A), we hypothesized that IL-3 negatively regulates the RNA binding potential of Hsc70. As a test, we compared the binding of radiolabeled Bim 3′UTR mRNA to immunoprecipitated Hsc70 protein complexes isolated from Baf-3 cells cultured with or without IL-3. Hsc70 protein was recovered efficiently from IL-3-treated or -untreated cells by immunoprecipitation (Figure 4B, lanes 1 and 2), and complexes of Bim mRNA bound to immunoprecipitated Hsc70 formed less efficiently in the presence of IL-3 than in its absence (Figure 4C). In contrast, binding of c-*fos* mRNA to immunoprecipitates did not vary in the presence or absence of IL-3 (right panel).

Immunoblots were used to test whether cochaperones that associate with Hsc70 (Bag family proteins, CHIP, Hip, and Hsp40, reviewed in Mayer and Bukau [2005]) mediate the IL-3 sensitivity of Hsc70 binding to Bim mRNA. Bag-1, -2, and -4 and CHIP, Hip, and Hsp40 were all detected in Baf-3 cell lysates. Of these, only Bag-4 steady-state levels were higher in IL-3-treated cells (Figure 4B, top row). When immunoblots of Hsc70 immunoprecipitates were analyzed with the same antibodies, all cochaperones except Bag-2 were detected (second row). Furthermore, the relative amounts of Bag-4 and CHIP that coprecipitated with Hsc70 increased in IL-3-treated cells, while those of Hsp40 and Hip decreased. By comparing the cochaperone signal strengths of Hsc70-bound or -unbound fractions, we estimate that 90% of Bag-4 coprecipitated with Hsc70, while only less than 10% of CHIP, Hip, or Hsp40 was present in Hsc70 immunocomplexes.

A cytosol-free system was used to test whether CHIP, Hip, or Hsp40 affect the RNA binding potential of Hsc70. In immunoblots with anti-Hsc70, the signal from purified Hsc70 bound to Bim mRNA-coated beads did not exceed background; however, addition of purified Hsp40 (DjB1) or Hip to the RNA binding reactions enhanced Hsc70 binding more than 4-fold (Figure 4D). Addition of both Hsp40 and Hip to the reactions did not further increase Hsc70 binding affinity to RNA, suggesting that these cochaperones enhance the stability of Hsc70 binding to RNA through common molecular mechanisms. In contrast, CHIP did not increase the recovery of Hsc70 from the RNA column but reversed Hsp40 and Hip stabilization of Hsc70-Bim mRNA complexes. These results support evidence that cochaperones bound to Hsc70 regulate the RNA binding potential of the Hsc70-protein complex.

Bag-4 and Hsp40 Control Baf-3 Cell Survival by Regulating Bim Expression

Baf-3 cell lines that overexpress Bag-4 were established. In one representative clone #17, steady-state levels of Bag-4 protein levels were maintained, in contrast to parent Baf-3 cells, in which Bag-4 declined after IL-3 starvation (Figure 4E). Extracts made from clone #17 cells cultured in the absence of IL-3 also induced more rapid deadenylation and degradation of Bim mRNA in vitro than control cell extracts (Figure 5A). Induction of Bim mRNA by IL-3 starvation is suppressed in Bag-4-overexpressing cells (Figures 5B and 5C). Bim protein induction was also attenuated (Figure 5D), although not as prominently as in Hsc70 knockdown cells (Figures 3D–3F). Consistent with these data, Bag-4-overexpressing cells continued to divide and survived longer than Baf-3 parent cells in IL-3-free medium (Figure 5E).

Steady-state levels of Bag-4 mRNA from early undifferentiated hematopoietic progenitors (Sca-1$^+$c-Kit$^+$Lin$^-$ from mouse primary bone marrow cultures) that proliferate in a SCF- and TPO-dependent manner (Kuribara et al., 2004) were measured by using qRT-PCR. Bag-4 mRNA levels declined when these cells were deprived of cytokines (Figure 4F), suggesting that cytokine-mediated survival of progenitor cells may involve Bag-4 control of mRNA stability.

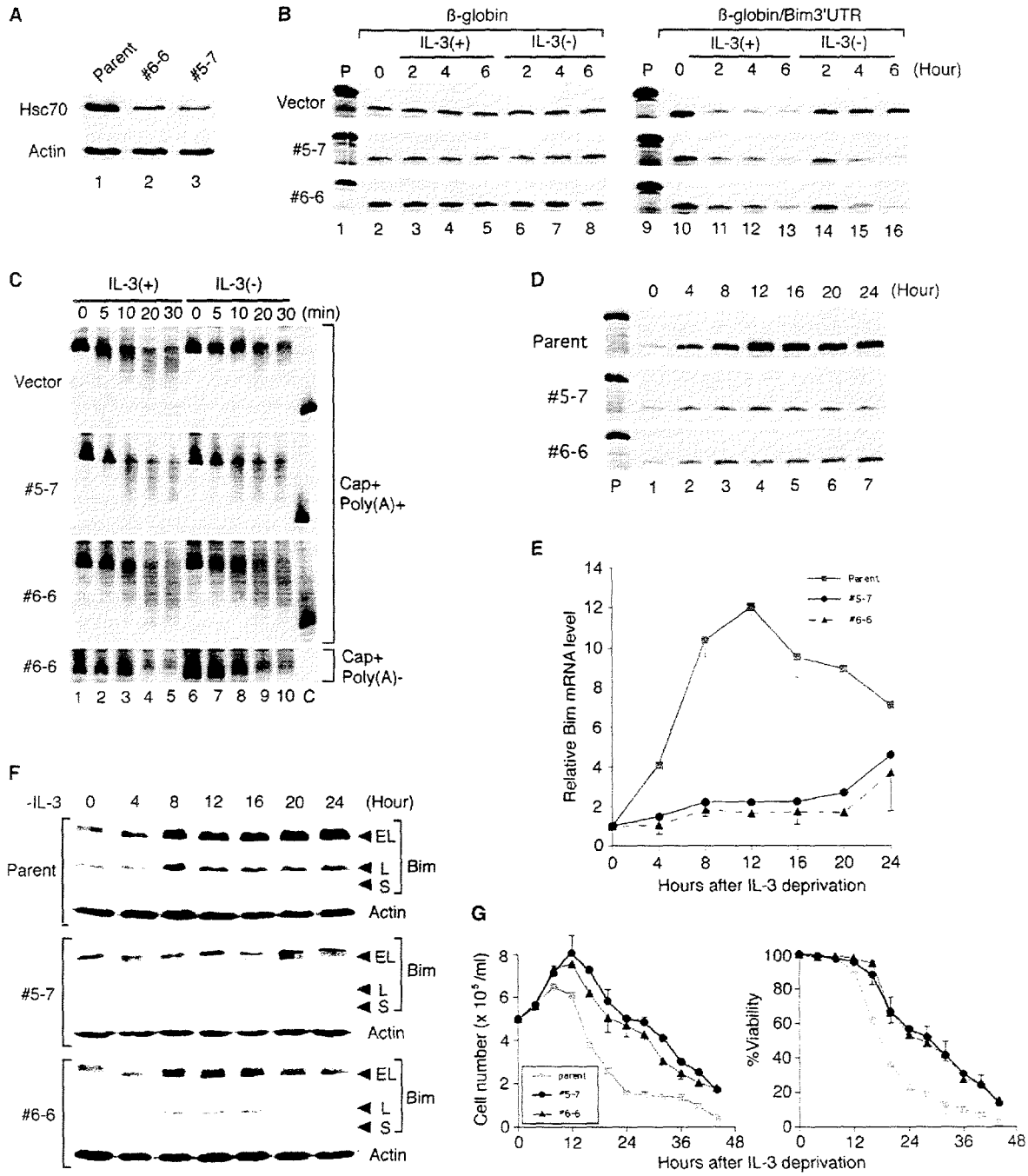

Figure 3. Effects of Hsc70 on mRNA Stability

(A) Immunoblot analysis of lysates from parent Baf-3 cells and representative lines expressing shRNAs that target different sequences in Hsc70 mRNA with Hsc70 or β-actin antibody.

(B) The stabilities of human β-globin mRNA or a β-globin/Bim (3'UTR) fusion mRNAs expressed transiently in two Hsc70 knockdown clones (and control cells with the piGENE-mU6 vector) cultured either in the presence or absence of IL-3. Message levels were measured using RPA.

(C) RNA-stability assay in vitro. Cytosol preparations from two Hsc70 knockdown clones and the negative control cells cultured in the presence or absence of IL-3 were incubated for indicated periods with radiolabeled and capped Bim mRNA with (top and middle panels) or without (bottom panel) a poly(A) tail of 100 residues.

(D–G) Parental Baf-3 cells and two Hsc70 knockdown lines were cultured without IL-3 for indicated periods. Bim mRNA expression was measured using RPA (D) or qRT-PCR (E). Bim and control β-actin protein expression (F), cell number (left), and viability (right) (G) are also shown. The mean and SD of three independent experiments are shown (E and G).

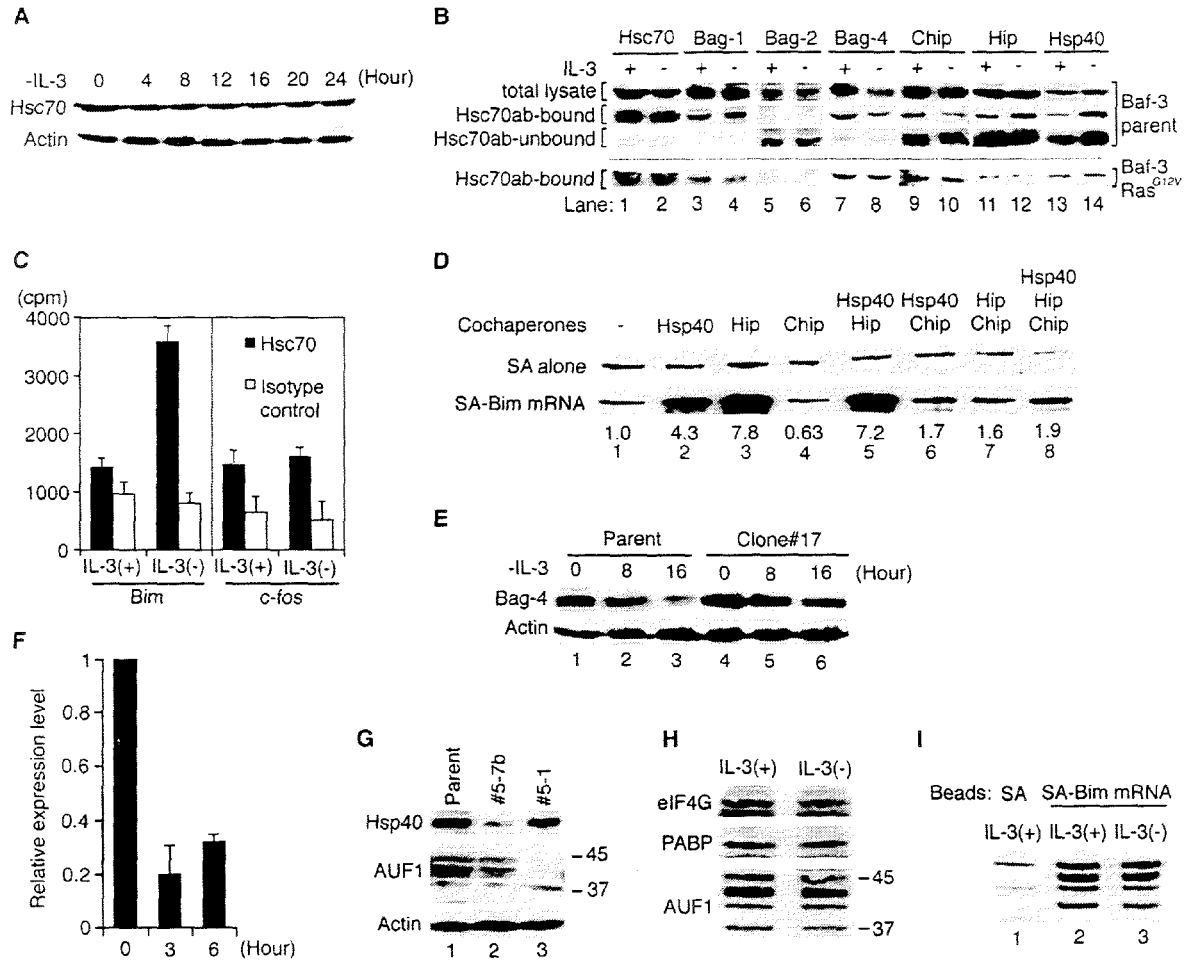

Figure 4. Cochaperones and RNA Binding Proteins Binding to Hsc70

(A) Hsc70 and β-actin protein levels in Baf-3 cells cultured without IL-3 for the times indicated.

(B) Cell extracts prepared from parent Baf-3 cells (upper three panels) or cells expressing Ras^{G12V} (bottom panels) cultured in the presence or absence of IL-3. Levels of individual proteins visualized by immunoblots of Baf-3 lysates with specific cochaperone antibodies marked above (top panels). Following immunoprecipitation, Hsc70 antibody-bound (upper middle and bottom panels) and Hsc70 antibody-unbound (lower middle panels) proteins were detected by immunoblotting. Equivalent cell numbers were analyzed.

(C) Immunoprecipitates with either Hsc70 antibodies or isotype control immunoglobulins were incubated with radiolabeled Bim (left) or c-fos (right) mRNAs. The amount of RNA bound to the beads was measured using a scintillation counter. The mean ± SD of three independent experiments is shown.

(D) Streptavidin beads (SA) alone or preincubated with biotinylated Bim mRNA (SA-Bim mRNA) were mixed with purified Hsc70 protein alone (lane 1) or Hsc70 with the cochaperones indicated above. Bead-bound Hsc70 protein was detected by immunoblot analysis. For each lane, the quantity of Hsc70 bound to SA-Bim mRNA relative to lane 1 is shown below.

(E) Parental Baf-3 cells and cells overexpressing Bag-4 (Clone #17) were cultured without IL-3 for the indicated periods. Immunoblot analyses with Bag-4 and β-actin antibodies are shown.

(F) Relative levels of Bag-4 mRNA were measured by qRT-PCR in murine early hematopoietic progenitors ($Sca1^+cKit^+Lin^-$) cultured in SCF- and TPO-free medium for the indicated periods. The mean and SD of three independent experiments are shown.

(G) Immunoblot analysis of Hsp40, AUF1, and β-actin by using lysates from parent Baf-3 cells or from representative lines #5-7b and #5-1, which express shRNAs targeting Hsp40 or AUF1 mRNA, respectively.

(H) Cytosol extracts of Baf-3 cells cultured with or without IL-3 were used in immunoprecipitations with Hsc70 antibody and then analyzed in immunoblots with antibodies against eIF4G, PABP, or AUF1.

(I) Streptavidin beads (SA) alone (lane 1) or those incubated with biotinylated Bim mRNA (SA-Bim mRNA; lanes 2 and 3) were mixed with cytosol from Baf-3 cells cultured with or without IL-3. Bead-bound AUF1 protein was detected by immunoblot analysis.

Hsp40 (DjB1) protein levels were reduced in Baf-3 clones expressing an Hsp40-specific shRNA (clone #5-7b, Figure 4G). In in vitro RNA decay assays, these cells showed mild enhancement of Bim mRNA deadenylation (Figure 5A), which correlates well with the mild suppression of Bim mRNA induction that occurs with IL-3

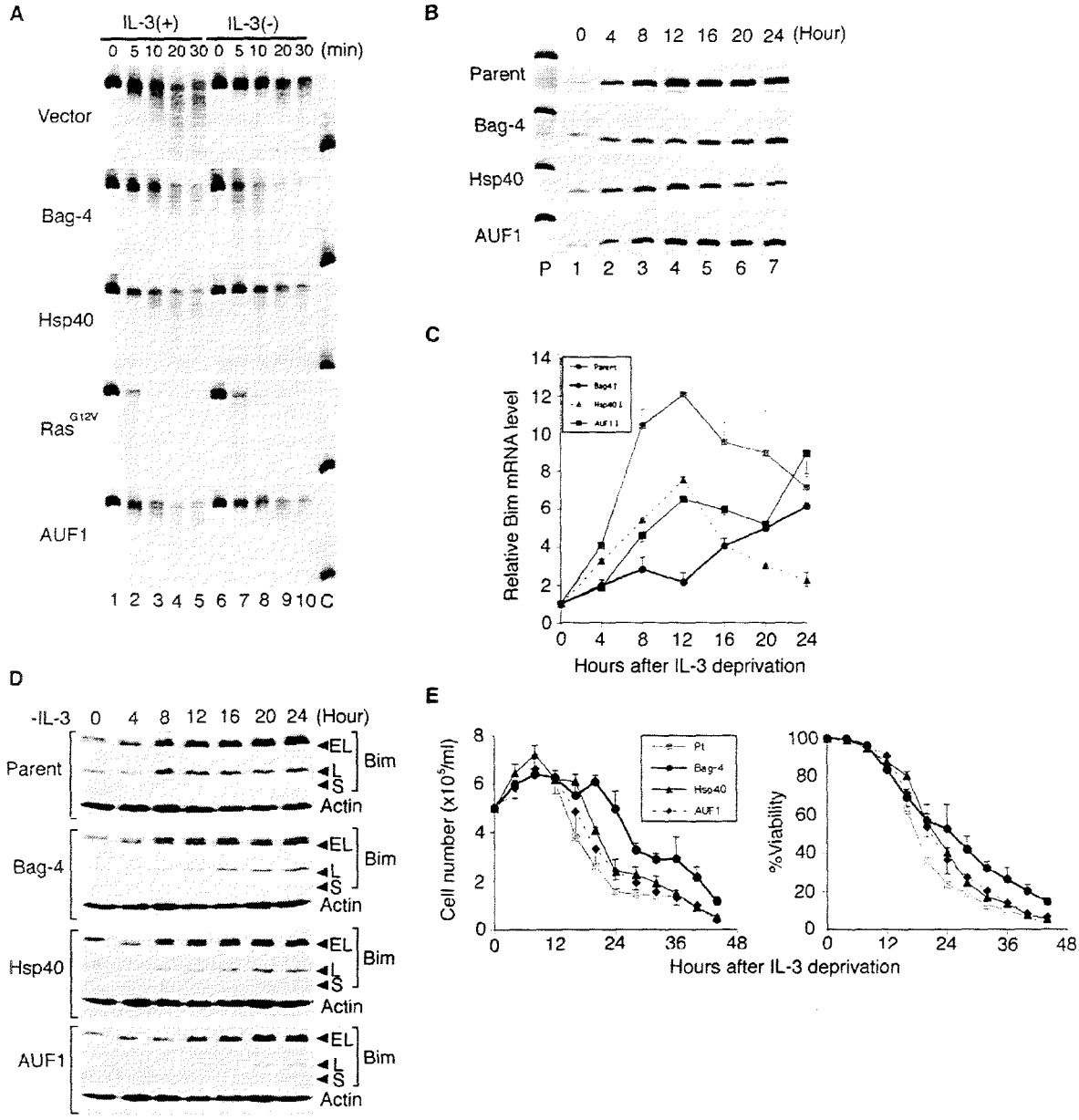

Figure 5. Effects of Hsc70 Binding Proteins on Bim Expression

Control Baf-3 cells transfected with the empty piGENE-mU6 vector, Bag-4-overexpressing clone #17, Hsp40 knockdown clone #5-7b, Ras^{G12V}-overexpressing cells, and AUF1 knockdown clone #5-1 were cultured with or without IL-3.

(A) RNA-stability assays in vitro using radiolabeled and capped Bim mRNA with a poly(A) tail of 100 residues.

(B–E) Cells were cultured without IL-3 for the times indicated above. Bim mRNA expression was analyzed using (B) ribonuclease protection assays, as well as (C) qRT-PCR. (D) Bim and β-actin protein expression. (E) Cell number (left) and viability (right). The mean and SD of three independent experiments are shown (C and E).

starvation (Figures 5B and 5C). However, Bim protein levels did not change (Figure 5D), and cell survival in the absence of IL-3 did not improve significantly (Figure 5E). Attempts to establish Baf-3 cell lines that overexpress CHIP or express Hip shRNA were not successful.

Hsp70 Fails to Substitute for Hsc70 as a Bim mRNA Stabilizer

Despite previous reports of heat-inducible Hsp70 binding to AREs (Henics et al., 1999; Zimmer et al., 2001; Wilson et al., 2001), Hsp70 was not detected among proteins

bound to Bim RNA on columns exposed to lysates of Baf-3 cells grown in the presence or absence of IL-3 (Figure 2D). To determine whether this is caused by the low expression level of Hsp70 in Baf-3 cells (Figure 6A, lanes 1 and 2) or inability of Hsp70 to bind to Bim mRNA, we tested Hsp70's RNA binding potential directly in a cytosol-free system. We detected no significant binding of Hsp70 to Bim mRNA either alone or in the presence of Hsp40 and Hip (Figure 6B). UV-crosslinking assays showed that recombinant Hsp70 with Hsp40 and Hip bound to *c-fos* mRNA, but not to Bim mRNA (Figure 6C). Potential of Hsp70 to stabilize Bim mRNA in the absence of Hsc70 was tested by using Baf-3 cells with Hsc70 levels reduced by shRNA expression (clone #6-6) and also expressed Hsp70 constitutively (#6-6+Hsp70 #1 and #3, Figure 6A). In in vitro mRNA decay assays, lysates from these clones grown in the presence or absence of IL-3, showed poor stabilization of Bim mRNA (Figure 6D). Consistent with these results, there was no increase in Bim protein levels in IL-3-starved cells (Figure 6E), and the survival of these lines was prolonged in the absence of IL-3 relative to Baf-3 parent cells (Figure 6F). These results indicate that Hsp70 does not bind to Bim mRNA and cannot substitute for Hsc70 in the stabilization of Bim mRNA.

Ras^{G12V} Regulates the Binding Potentials of Cochaperones to Hsc70 and Destabilizes Bim mRNA

Previous reports established that Ras-activated pathways play a critical role in the transduction of survival signals from cytokine receptors (reviewed by Inaba [2004]). When starved for IL-3, Baf-3 cells expressing constitutively active Ras (Ras^{G12V}) show no induction of Bim mRNA, and cells live indefinitely in IL-3-free medium. In in vitro Bim mRNA decay assays, Bim mRNA was rapidly deadenylated in extracts of Baf-3 cells expressing Ras^{G12V} in the absence or presence of IL-3 (Figure 5A).

To investigate what components may be involved in this extremely rapid mRNA decay, the Hsc70/cochaperone complex formed in Baf-3 cells expressing Ras^{G12V} was examined by immunoblot analysis of Hsc70 immunoprecipitates with cochaperone-specific antibodies. Levels of cochaperones associated with Hsc70 were the same in Baf-3 cells grown in the absence or presence of IL-3 (Figure 4B, bottom panels), and Bag-4, CHIP, and Hsp40 levels were similar to those observed in parent Baf-3 cells cultured with IL-3. One possible contribution to the very rapid decay of Bim mRNA may be the levels of Hsc70-bound Hip protein, which were reduced in cells expressing Ras^{G12V} relative to parent cells cultured with IL-3.

Hsc70 Forms a Complex with eIF4G, PABP, and AUF1

Hsc70 interacts with AUF1, an ARE binding protein that regulates RNA stability and forms a ternary complex with eIF4G/eIF4E (translation initiation factors that bind to the cap) and poly(A) binding protein (PABP) (Laroia et al., 1999; Grosset et al., 2000). In coimmunoprecipitation assays from extracts of Baf-3 cells cultured with or without IL-3, there were similar levels of eIF4G, PABP and four alternative spliced isoforms of AUF1 (p37, p40, p42, and p45) in complex with Hsc70 (Figure 4H).

Unlike Hsc70 (Figure 2), the recovery of AUF1 with Bim mRNA-coated beads did not vary in cytosol extracts prepared from Baf-3 cells cultured in the presence or absence of IL-3 (Figure 4I). The role of AUF1 in Bim mRNA stability was investigated in Baf-3 cells expressing AUF1 shRNA. Although all forms of AUF1 except p37 were less abundant in clone #5-1 (Figure 4G), AUF1 downregulation had little or no effect on Bim mRNA decay (Figure 5A), steady-state levels of Bim mRNA (Figures 5B and 5C) or Bim protein (Figure 5D), or cell growth and survival in the absence of IL-3 (Figure 5E). These results suggest a limited role for AUF1 in the regulation of Bim mRNA stability.

DISCUSSION

In earlier studies, we and others demonstrated that regulation of Bim and p27 steady-state mRNA levels by cytokines contributes to homeostasis of blood cell number. Here we demonstrate that cytokines shorten the half-life of Bim mRNA by reducing the RNA binding affinity of Hsc70, an mRNA-stabilizing factor. We propose the following model for cytokine-mediated control of Bim mRNA (Figure 7). In the presence of IL-3, Hsc70 protein that is associated with Bag-4 and CHIP has little RNA binding potential. As a result, Bim mRNA is more likely to be bound by a RNA-destabilizing factor(s), which targets Bim mRNA for degradation by ribonucleases. In the absence of IL-3, Hsc70 binds preferentially to Hsp40 and Hip. The association of this complex (with eIF4G and PABP) with Bim mRNA protects it from ribonucleases. Aspects of this model also apply to the cytokine-dependent regulation of p27 mRNA.

AUF1 is a target of ubiquitin-protease pathways that contributes to the rapid turnover of ARE-containing mRNAs (Laroia et al., 1999). As a component of the Hsc70 complex (Figure 4H) that was detected in Baf-3 cells by Bim RNA-affinity chromatography (Figure 4I), AUF1 is a candidate Bim mRNA destabilizer. However, interactions between AUF1 and Hsc70 or Bim mRNA did not change by IL-3 (Figures 4H and 4I). Moreover, shRNA-mediated downregulation of AUF1 did not alter Bim mRNA stability (Figures 5A–5C). Among the four alternatively spliced variants, $p37^{AUF1}$ is the major ubiquitinated isoform that contributes to rapid degradation of mRNA (Laroia and Schneider, 2002; Sarkar et al., 2003). Because we failed to downregulate this isoform (Figure 4G), we overexpressed $p37^{AUF1}$ in Baf-3 cells, and again little effect was observed (data not shown). These findings support a model in which an mRNA-destabilization factor(s) other than AUF1 plays a critical role in the rapid decay of Bim mRNA in IL-3-treated Baf-3 cells.

We demonstrated previously that activation of Ras pathways is essential for the downregulation of Bim mRNA and the long-term survival of Baf-3 cells (Kuribara

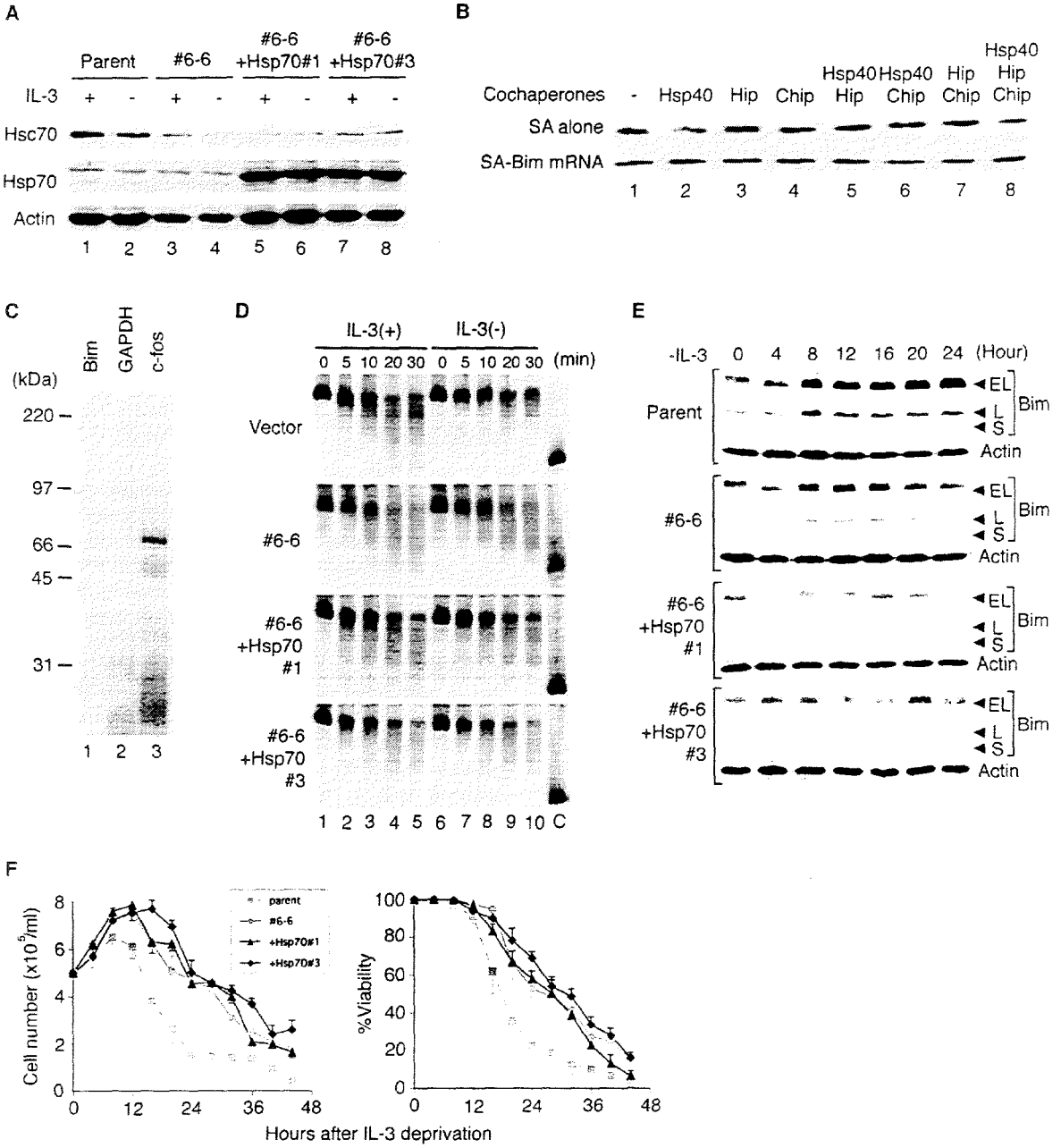

Figure 6. Inability of Hsp70 to Stabilize Bim mRNA

(A) Immunoblot analysis of Hsc70 (top panel), Hsp70 (middle panel), and β-actin (bottom panel) in lysates from parent Baf-3 cells, Hsc70 knockdown clone #6-6, and two representative lines from #6-6 that express Hsp70 constitutively.

(B) Streptavidin beads (SA) alone (top panel) or preincubated with biotinylated Bim mRNA (SA-Bim mRNA; bottom panel) were mixed with purified Hsp70 protein alone (lane 1) or with the cochaperones indicated above. Bead-bound Hsp70 protein was detected by immunoblot analysis.

(C) UV-crosslinking assay. Mixtures of recombinant Hsp70, Hsp40, and Hip were incubated with radiolabeled Bim, GAPDH, or c-*fos* mRNA.

(D–F) Parent Baf-3 cells, clone #6-6, and two clones from #6-6 expressing Hsp70 were cultured with or without IL-3 for indicated periods. RNA stability assay in vitro, using capped Bim mRNA with a poly(A) tail (D), Bim and β-actin protein expression (E), and the mean and SD of cell number (left) and viability (right) in three independent experiments (F) are shown.

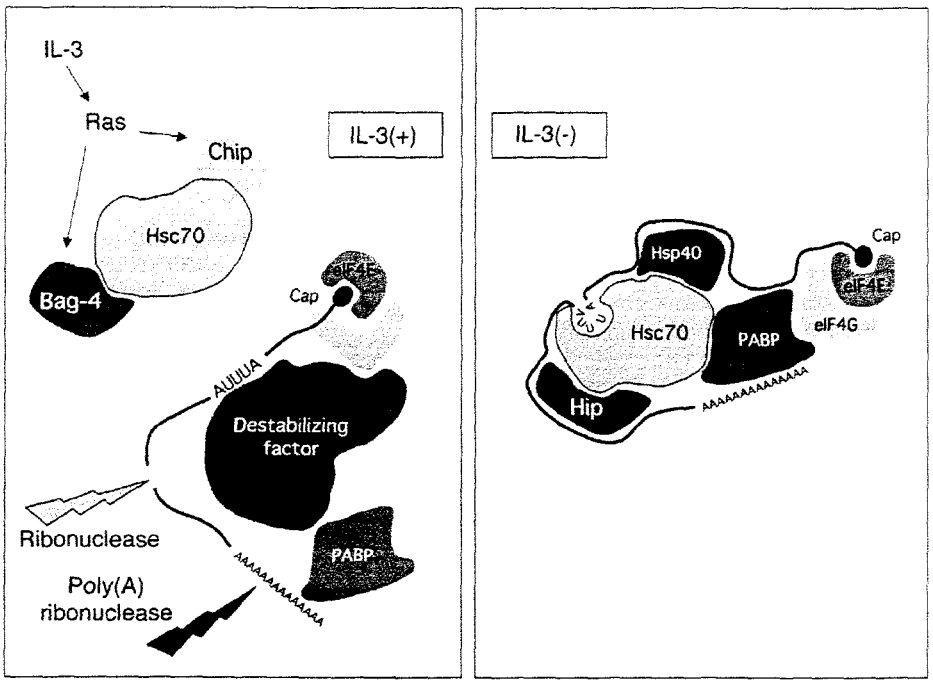

Figure 7. Model for the Cytokine-Dependent Regulation of mRNA Stability
In the presence of IL-3, Hsc70 associated with Bag-4 and CHIP has a low affinity for RNA. Bim mRNA, which preferentially binds to RNA destabilizing factor(s), is a target for ribonucleases. In the absence of IL-3, an Hsc70/Hsp40/Hip complex associated with eIF4G and PABP forms a high-stability complex with Bim mRNA that protects it from ribonucleases.

et al., 1999; Shinjyo et al., 2001). Consistent with these data, induced expression of Ras^{G12V} resulted in extremely rapid decay of Bim mRNA (Figure 5A) and bypassed the requirement for IL-3 as a regulator of Hsc70 binding to Bag-4, CHIP, Hip, or Hsp40 (Figure 4B). Thus, we hypothesize that these cochaperones (and possibly others) function *cooperatively* in responding to cytokine-dependent survival signals by regulating Hsc70's RNA binding potential. Our finding that changes in the steady-state levels of a single cochaperone affect Bim mRNA expression less than downregulation of Hsc70 itself support this hypothesis. We are currently investigating a molecular mechanism(s) by which IL-3 and Ras^{G12V} regulate CHIP, Hip and Hsp40 binding to Hsc70.

Previous reports of the RNA binding potential of Hsc70 and Hsp70, which bind directly to native AREs as well as artificial AUUUA-containing RNAs, illustrate few differences between these two chaperones (Henics et al., 1999; Zimmer et al., 2001; Wilson et al., 2001). In contrast, we found that, unlike Hsc70, Hsp70 binds well to the c-*fos* ARE and only weakly to Bim mRNA in the presence of Hsp40 and/or Hip (Figures 6B and 6C). Hsp70 also failed to substitute for Hsc70 as a Bim mRNA stabilizer (Figures 6D–6F). Theologically, any model involving Hsp70 binding directly to Bim mRNA would promote cell killing instead of protecting cells in stressful conditions.

Hsp70 family chaperones share common structural motifs including a 45 kDa N-terminal ATPase domain and a 23 kDa C-terminal substrate binding domain composed of a β sandwich and α helix subdomains (Zhu et al., 1996). Although Hsp70 and Hsc70 amino acids are nearly 90% identical in the ATPase domain and β sandwich subdomain, identity in the α helix subdomain is only 65% identical. The ATPase domain has been determined to be sufficient for ARE binding, but the substrate binding domain is required for RNA binding fidelity and sequence preference (Zimmer et al., 2001). Thus, divergence in the α helix subdomains of Hsc70 and Hsp70 could target the specificities of these proteins binding to Bim and c-*fos* mRNAs, respectively. Because the AREs of Bim, p27, and c-*fos* are all classified as "WAUUUAW and U-rich region" motifs (W stands for A or U) (reviewed in Wilusz et al. [2001]), it is conceivable that α helix subdomains may distinguish *cis* elements other than AUUUA within AREs that are currently unidentified.

Although Hsp70's α helix subdomain is likely to play an important role in gene-specific RNA binding of chaperones, differences in the protein band patterns resulting from Bim/p27, GAPDH, and c-*fos* RNA-affinity chromatography and UV-crosslinking assays (Figures 2A and 2F) suggest contributions of other 3′UTR binding proteins. It should also be noted that although AREs play a critical role as protein docking sites, non-ARE flanking sequences may also function as *cis*-acting regulatory elements that further specify the binding potential of Hsc70 to AREs. A recent report of CA repeats that mediate constitutive

degradation of Bcl-2 mRNA (Lee et al., 2004) suggests involvement of non-ARE sequences in the control of mRNA stability.

Because Bim plays a critical role in the regulation of hematopoietic cell number (Bouillet et al., 1999), altered regulation of Bim could be involved in leukemogenesis. Negative regulation of Bim by the Bcr-Abl chimeric kinase has been shown to contribute to an increase in white blood cell and hematopoietic progenitor counts in the chronic phase of chronic myelogenous leukemia (CML) (Kuribara et al., 2004; Aichberger et al., 2005). At least part of the inhibition of leukemic blast proliferation provided by antileukemic drugs such as imatinib mesylate or AMN107 (which target Bcr-Abl kinase) is due to increased levels of Bim protein (Kuribara et al., 2004; Aichberger et al., 2005; Fiskus et al., 2006). Because negative regulation of Bim by Bcr-Abl may be mediated by Hsc70 and associated cochaperones, our laboratory endeavors to understand the formation and regulation of this complex as a means to identify new molecular targets for antileukemic drugs.

EXPERIMENTAL PROCEDURES

Cells and Cell Culture

IL-3-dependent cells were cultured as described previously (Shinjyo et al., 2001). The piGENE-mU6 vector (Miyagishi et al., 2004) was used for expression of shRNAs with sequences targeting Hsc70#5, UGAGGGAAUUGACUUCUAUAC; Hsc70#6, UGAUGCUGUUGUUCAGUCUGA; Hsp40#5, GUGGAGACCUUGUUAUCGAGU; or AUF1#5, ACAAUGUUGGUCUUAGUAAAU. Bag-4 and Hsp70 overexpression lines were established by standard procedures (Shinjyo et al., 2001). At least three independent clones were isolated and analyzed. Baf-3 cells expressing Ras^{G12V} were a gift from Dr. Atsushi Miyajima. Murine undifferentiated early hematopoietic progenitors ($Sca\text{-}1^+c\text{-}Kit^+Lin^-$) were isolated and cultured as previously described (Kuribara et al., 2004).

Measurements of mRNA Stability

mRNA stability in vivo was measured using the Tet-inducible expression system as previously described (Xu et al., 1998). Native and hybrid human β-globin mRNAs were detected by RPA or by qRT-PCR with primers 5′-GGGATCTGTCCACTCCTGATGCTG-3′ in exon 2 and 5′-ATGGGCCAGCACACAGACCAGCAC-3′ in exon 3. Half-lives of in vitro-synthesized mRNAs incubated with cytosolic (S100) cell extracts were analyzed as described previously (Ford and Wilusz, 1999). Target mRNAs included the Bim 3′UTR region conserved between human and mouse, or the complete 3′UTRs of p27 and *c-fos*. Short target mRNA sequences were as follows: Bim, UAACUUGUAGAGAUGUUGUAUAUUUAUUUUCCGCUUAUUUAAAUGUCUUAAGUUCUUGAAA; p27, AAAAUUAUACUAACUUAUUUAUGUUAAAAAGAGAUUUUUUUUUAAUCUAGACAAUAUACAA; and GAPDH, CCCUGGACCACCCACCCCAGCAAGGACACUGAGCAAGAGAGGCCCUAUCCCAACUCGGCCC. Radiolabeled, capped (^{7Me}GpppG) mRNAs synthesized in vitro with or without a 100 bp poly(A) tail were incubated at 37°C with S100 extracts. Signals from mRNAs resolved on 5% acrylamide gels containing 7 M urea were quantified using a Bas3000 phosphoimager (Fuji, Tokyo, Japan).

Enrichment and Identification of RNA Binding Proteins

RNA-affinity chromatography was performed as described (Skalweit et al., 2003). Briefly, biotinylated mRNAs encoding the 3′UTR of Bim, GAPDH, p27, or c-*fos* mRNA and bound to streptavidin-coated agarose beads were exposed to S100 extracts for 45 min at 4°C and then for 15 min at room temperature. Protein-bound beads were washed gently (150 mM KCl, 1.5 mM $MgCl_2$, 10 mM Tris [pH 7.5], 0.5 mM DTT). Bound proteins were then released by boiling in SDS sample buffer, resolved by SDS-PAGE, and visualized by silver staining or immunoblot analysis. Protein bands of interest were recovered and analyzed using a matrix-assisted laser desorption/ionization time-of-flight (MALDI-TOF/TOF) tandem mass spectrometer (Ultraflex, Bruker, Bremen, Germany).

In Vitro RNA Binding Assay

Hsc70 protein complexes, isolated and eluted from an Hsc70 antibody (1B5, Stressgen, Victoria, Canada) bound to protein G beads, were incubated with in vitro-synthesized radiolabeled mRNA in RNA binding buffer (10 mM MOPS [pH 7.2], 50 mM KCl, 3 mM $MgCl_2$, 0.5 mM ATP, 2 mM DTT) containing RNase OUT (Invitrogen, Carlsbad, California) at 37°C for 30 min. After washing, bead-bound RNA was quantified using a scintillation counter. For cytosol-free RNA binding assays, 10 μg of in vitro-synthesized biotinylated Bim mRNA bound to streptavidin-coated beads was incubated with 500 ng Hsc70 (with or without an equimolar concentration of Hsp40, Hip, or CHIP) in RNA binding buffer at 4°C for 45 min and then at room temperature for 15 min. After washing the beads, bound proteins were released by boiling in SDS sample buffer and were subjected to immunoblot analysis.

RNA gel retardation assays were performed as described (Mahtani et al., 2001). Briefly, Hsc70 (with or without Hsp40 and/or Hip) were preincubated with or without 1 μl of Hsc70 (SPA-816, Stressgen) or Hsp40 antiserum for 30 min on ice. Radiolabeled RNA probe (derived from the human Bim 3′UTR, 5′-UCUGUGUGAUGUGUCCUACUGUUUCAUAAUGCUGUAACUUGUAGAAAUAUUGUAUAUUUAUUUUCUGCUUAUUUAAUGUCUUAAUUUCUGAAA-3′) in RNA binding buffer (20 mM HEPES [pH 7.6], 3 mM $MgCl_2$, 40 mM KCl, 2 mM DTT, and 5% glycerol), RNase T1 (25 U/ml), and heparin sulfate (5 mg/ml) were added, and the mixture was incubated on ice for 20 min. The resulting binding reactions were resolved by electrophoresis on a nondenaturing 4% polyacrylamide gel run at 150 V for 3 hr at 4°C.

UV-crosslinking assay was performed as described (Chen et al., 2000) with modification. Mixtures of recombinant proteins or cytoplasmic extracts (20 μg protein) were incubated with ^{32}P-labeled RNA (0.5 ng = 2 × 10^5 cpm) at room temperature for 20 min in 10 μl of RNA binding buffer containing 1 μg heparin. Reaction mixtures were transferred to a 96-well plate and irradiated for 10 min on ice with a UV Stratalinker (Invitrogen) at a distance of 5 cm. Unbound RNA was then digested with RNase A (200 ng) for 10 min at 37°C, and samples were resolved by SDS-PAGE (10%). Probes were as follows: for Bim or GAPDH, the same as used in gel retardation assays or in vitro mRNA decay assays, respectively; for *c-fos*, 5′-UUUUAUUGUGUUUUUAUUUAUUUAUUAAGAUGGAUUCUCAGAUAUUUAUAUUUUUAUUUUAUUUUUUU-3′.

Other Experimental Procedures and Reagents

qRT-PCR was performed with exon 1-exon 2 primer sets: 5′-AATGTCTGACTCTGATTCTCGGAC-3′ and 5′-TCTCAGCAGGCTGCAATTGTCCAC-3′ for Bim and 5′-GCAGGTGGCGATGGCTACTACCCC-3′ and 5′-CCATTTGCATAAGAATTCAGGCTC-3′ for Bag-4, and 28S ribosomal RNA as an internal control (Kuribara et al., 2004). Antibodies included anti-actin (1378 996, Roche, Mannheim, Germany); anti-AUF1 (07-260) and -SODD (Bag-4, 07-092) from Upstate Cell Signaling Solutions (Lake Placid, New York); anti-Bag-1 (FL-274), -Hsc70 (B-6), and -p27 (C-19) from Santa Cruz Biotechnology (Santa Cruz, California); anti-Bag-2 (Oxford Biotechnology, Oxfordshire, United Kingdom); Chip (Ab-1, Oncogene Research Products (San Diego, California); anti-eIF4G1 (BL896, Bethyl laboratories, Montgomery, Texas); and anti-Hip (SPA-766), -Hsp40 (SPA-400), and -Hsp70 (C92F3A-5) from Stressgen. A rabbit anti-PABP was raised against a GST-mouse PABP (aa 213–422) fusion protein, and anti-Bim antibodies were described elsewhere (Shinjyo et al., 2001). Recombinant Hsc70, Hsp70, and Hsp40 (DjB1) proteins were from Stressgen. Hexameric

His-tagged mouse Hip protein was expressed in *E. coli* using the pQE-80L vector (Qiagen, Hilden, Germany) and purified using Ni-NTA beads. Mouse CHIP protein was synthesized as a GST fusion and cleaved by thrombin.

ACKNOWLEDGMENTS

This work was supported by Grants-in-Aid for Scientific Research from the Ministry of Education, Culture, Sports, Science, and Technology of Japan.

Received: August 8, 2006
Revised: November 5, 2006
Accepted: December 12, 2006
Published: January 11, 2007

REFERENCES

Aichberger, K.J., Mayerhofer, M., Krauth, M.T., Vales, A., Kondo, R., Derdak, S., Pickl, W.F., Selzer, E., Deininger, M., Druker, B.J., et al. (2005). Low-level expression of proapoptotic Bcl-2-interacting mediator in leukemic cells in patients with chronic myeloid leukemia: role of BCR/ABL, characterization of underlying signaling pathways, and reexpression by novel pharmacologic compounds. Cancer Res. *65*, 9436–9444.

Akiyama, T., Bouillet, P., Miyazaki, T., Kadono, Y., Chikuda, H., Chug, U., Fukuda, A., Hikita, A., Seto, H., Okada, T., et al. (2003). Regulation of osteoclast apoptosis by ubiqutination of proapoptotic BH3-only Bcl-2 family member Bim. EMBO J. *22*, 6653–6664.

Birkenkamp, K.U., and Coffer, P.J. (2003). Regulation of cell survival and proliferation by the FOXO (Forkhead box, class O) subfamily of Forkhead transcription factors. Biochem. Soc. Trans. *31*, 292–297.

Bouillet, P., Metcalf, D., Huang, D.C.S., Tarlinton, D.M., Kay, T.W.H., Koentgen, F., Adams, J.M., and Strasser, A. (1999). Proapoptotic Bcl-2 relative Bim required for certain apoptotic responses, leukocyte homeostasis, and to preclude autoimmunity. Science *286*, 1735–1738.

Chen, C.Y., Gherzi, R., Andersen, J.S., Gaietta, G., Jurchott, K., Royer, H.D., Mann, M., and Karin, M. (2000). Nucleolin and YB-1 are required for JNK-mediated interleukin-2 mRNA stabilization during T-cell activation. Genes Dev. *14*, 1236–1248.

Dijkers, P.F., Medemadagger, R.H., Lammers, J.J., Koenderman, L., and Coffer, P.J. (2000a). Expression of the proapoptotic bcl-2 family member bim is regulated by the forkhead transcription factor FKHR-L1. Curr. Biol. *10*, 1201–1204.

Dijkers, P.F., Medema, R.H., Pals, C., Banerji, L., Thomas, N.S., Lam, E.W., Burgering, B.M., Raaijmakers, J.A., Lammers, J.W., Koenderman, L., et al. (2000b). Forkhead transcription factor FKHR-L1 modulates cytokine-dependent transcriptional regulation of p27(KIP1). Mol. Cell. Biol. *20*, 9138–9148.

Duttagupta, R., Vasudevan, S., Wilusz, C.J., and Peltz, S.W. (2003). A yeast homologue of Hsp70, Ssa1p, regulates turnover of the MFA2 transcript through its AU-rich 3′ untranslated region. Mol. Cell. Biol. *23*, 2623–2632.

Fero, M.L., Rivkin, M., Tasch, M., Porter, P., Carow, C.E., Firpo, E., Polyak, K., Tsai, L.H., Broudy, V., Perlmutter, R.M., et al. (1996). A syndrome of multiorgan hyperplasia with features of gigantism, tumorigenesis, and female sterility in p27(Kip1)-deficient mice. Cell *85*, 733–744.

Fiskus, W., Pranpat, M., Bali, P., Balasis, M., Kumaraswamy, S., Boyapalle, S., Rocha, K., Wu, J., Giles, F., Manley, P.W., et al. (2006). Combined effects of novel tyrosine kinase inhibitor AMN107 and histone deacetylase inhibitor LBH589 against Bcr-Abl expressing human leukemia cells. Blood *108*, 645–652.

Ford, L.P., and Wilusz, J. (1999). An in vitro system using HeLa cytoplasmic extracts that reproduces regulated mRNA stability. Methods *17*, 21–27.

Freeman, R.S., Burch, R.L., Crowder, R.J., Lomb, D.J., Schoell, M.C., Straub, J.A., and Xie, L. (2004). NGF deprivation-induced gene expression: after ten years, where do we stand? Prog. Brain Res. *146*, 111–126.

Gilley, J., Coffer, P.J., and Ham, J. (2003). FOXO transcription factors directly activate bim gene expression and promote apoptosis in sympathetic neurons. J. Cell Biol. *162*, 613–622.

Grosset, C., Chen, C.-Y.A., Xu, N., Sonenberg, N., Jacquemin-Sablon, H., and Shyu, A.-B. (2000). A mechanism for translationally coupled mRNA turnover: interaction between the poly(A) tail and a c-*fos* RNA coding determinant via a protein complex. Cell *103*, 29–40.

Henics, T., Nagy, E., Oh, H.J., Csermely, P., von Gabain, A., and Subjeck, J.R. (1999). Mammalian Hsp70 and Hsp110 proteins bind to RNA motifs involved in mRNA stability. J. Biol. Chem. *274*, 17318–17324.

Hohfeld, J., Minami, Y., and Hartl, F.U. (1995). Hip, a novel cochaperone involved in the eukaryotic Hsc70/Hsp40 reaction cycle. Cell *83*, 589–598.

Hsu, S.Y., Lin, P., and Hsueh, A.J. (1998). BOD (Bcl-2-related ovarian death gene) is an ovarian BH3 domain-containing proapoptotic Bcl-2 protein capable of dimerization with diverse antiapoptotic Bcl-2 members. Mol. Endocrinol. *12*, 1432–1440.

Inaba, T. (2004). Cytokine-mediated cell survival. Int. J. Hematol. *80*, 210–214.

Kuribara, R., Kinoshita, T., Miyajima, A., Shinjyo, T., Yoshihara, T., Inukai, T., Ozawa, K., Look, A.T., and Inaba, T. (1999). Two distinct interleukin-3-mediated signal pathways, Ras-NFIL3(E4BP4) and Bcl-xL, regulate the survival of murine pro-B lymphocytes. Mol. Cell. Biol. *19*, 2754–2762.

Kuribara, R., Honda, H., Matsui, H., Shinjyo, T., Inukai, T., Sugita, K., Nakazawa, S., Hirai, H., Ozawa, K., and Inaba, T. (2004). Roles of Bim in apoptosis of normal and Bcr-Abl-expressing hematopoietic progenitors. Mol. Cell. Biol. *24*, 6172–6183.

Laroia, G., and Schneider, R.J. (2002). Alternate exon insertion controls selective ubiquitination and degradation of different AUF1 protein isoforms. Nucleic Acids Res. *30*, 3052–3058.

Laroia, G., Cuesta, R., Brewer, G., and Schneider, R.J. (1999). Control of mRNA decay by heat shock-ubiquitin-proteasome pathway. Science *284*, 499–502.

Lee, J.H., Jeon, M.H., Seo, Y.J., Lee, Y.J., Ko, J.H., Tsujimoto, Y., and Lee, J.H. (2004). CA repeats in the 3′-untranslated region of bcl-2 mRNA mediate constitutive decay of bcl-2 mRNA. J. Biol. Chem. *279*, 42758–42764.

Ley, R., Balmanno, K., Hadfield, K., Weston, C.R., and Cook, S.J. (2003). Activation of the ERK1/2 signalling pathway promotes phosphorylation and proteasome-dependent degradation of the BH3-only protein Bim. J. Biol. Chem. *278*, 18811–18816.

Luciano, F., Jacquel, A., Colosetti, P., Herrant, M., Cagnol, S., Pages, G., and Auberger, P. (2003). Phosphorylation of Bim-EL by Erk1/2 on serine 69 promotes its degradation via the proteasome pathway and regulates its proapoptotic function. Oncogene *22*, 6785–6793.

Mahtani, K.R., Brook, M., Dean, J.L., Sully, G., Saklatvala, J., and Clark, A.R. (2001). Mitogen-activated protein kinase p38 controls the expression and posttranslational modification of tristetraprolin, a regulator of tumor necrosis factor alpha mRNA stability. Mol. Cell. Biol. *21*, 6461–6469.

Matsui, H., Shinjyo, T., and Inaba, T. (2005). Structure of the human Bim gene and its transcriptional regulation in Baf-3, interleukin-3-dependent hematopoietic cells. Mol. Biol. Rep. *32*, 79–85.

Mayer, M.P., and Bukau, B. (2005). Hsp70 chaperones: cellular functions and molecular mechanism. Cell. Mol. Life Sci. *62*, 670–684.

Leukemia (2007) 21, 288–296

www.nature.com/leu

ORIGINAL ARTICLE

Hypercalcemia in childhood acute lymphoblastic leukemia: frequent implication of parathyroid hormone-related peptide and *E2A-HLF* from translocation 17;19

T Inukai[1], K Hirose[1], T Inaba[2], H Kurosawa[3], A Hama[4], H Inada[5], M Chin[6], Y Nagatoshi[7], Y Ohtsuka[8], M Oda[9], H Goto[10], M Endo[11], A Morimoto[12], M Imaizumi[13], N Kawamura[14], Y Miyajima[15], M Ohtake[16], R Miyaji[17], M Saito[18], A Tawa[19], F Yanai[20], K Goi[1], S Nakazawa[1] and K Sugita[1]

[1]*Department of Pediatrics, University of Yamanashi, School of Medicine, Yamanashi, Japan;* [2]*Department of Molecular Oncology, Research Institute for Radiation Biology and Medicine, Hiroshima University, Hiroshima, Japan;* [3]*Department of Pediatrics, Dokkyo University School of Medicine, Tochigi, Japan;* [4]*Department of Pediatrics, Nagoya University Graduate School of Medicine, Nagoya, Japan;* [5]*Department of Pediatrics, Kurume University School of Medicine, Kurume, Japan;* [6]*Department of Pediatrics, Nihon University School of Medicine, Tokyo, Japan;* [7]*Section of Pediatrics, National Kyushu Cancer Center, Fukuoka, Japan;* [8]*Division of Cellular Therapy, Institute of Medical Science, University of Tokyo, Tokyo, Japan;* [9]*Department of Pediatrics, Okayama University Medical School, Okayama, Japan;* [10]*Department of Pediatrics, Yokohama City University School of Medicine, Yokohama, Japan;* [11]*Department of Pediatrics, Iwate Medical University School of Medicine, Morioka, Japan;* [12]*Department of Pediatrics, Kyoto Prefectural University of Medicine Graduate School of Medical Science, Kyoto, Japan;* [13]*Department of Hematology and Oncology, Miyagi Children's Hospital, Sendai, Japan;* [14]*Department of Pediatrics, Osaka Rosai Hospital, Sakai, Japan;* [15]*Section of Pediatrics, Anjo Kosei Hospital, Anjo, Japan;* [16]*Department of Pediatrics, Sendai City Hospital, Sendai, Japan;* [17]*Department of Pediatrics, University of Occupational and Environmental Health School of Medicine, Kitakyushu, Japan;* [18]*Department of Pediatrics and Adolescent, Juntendo University School of Medicine, Tokyo, Japan;* [19]*Section of Pediatrics, National Hospital Organization Osaka National Hospital, Osaka, Japan and* [20]*Department of Pediatrics, Fukuoka University School of Medicine, Fukuoka, Japan*

Hypercalcemia is relatively rare but clinically important complication in childhood leukemic patients. To clarify the clinical characteristics, mechanisms of hypercalcemia, response to management for hypercalcemia, incidence of t(17;19) and final outcome of childhood acute lymphoblastic leukemia (ALL) accompanied by hypercalcemia, clinical data of 22 cases of childhood ALL accompanied by hypercalcemia (>12 mg/dl) reported in Japan from 1990 to 2005 were retrospectively analyzed. Eleven patients were 10 years and older. Twenty patients had low white blood cell count ($<20 \times 10^9$/l), 15 showed hemoglobin $\geqslant 8$ g/dl and 14 showed platelet count $\geqslant 100 \times 10^9$/l. Parathyroid hormone-related peptide (PTHrP)-mediated hypercalcemia was confirmed in 11 of the 16 patients in whom elevated-serum level or positive immunohistochemistry of PTHrP was observed. Hypercalcemia and accompanying renal insufficiency resolved quickly, particularly in patients treated with bisphosphonate. t(17;19) or add(19)(p13) was detected in five patients among 17 patients in whom karyotypic data were available, and the presence of *E2A-HLF* was confirmed in these five patients. All five patients with t(17;19)-ALL relapsed very early. Excluding the t(17;19)-ALL patients, the final outcome of ALL accompanied by hypercalcemia was similar to that of all childhood ALL patients, indicating that the development of hypercalcemia itself is not a poor prognostic factor.
Leukemia (2007) **21**, 288–296. doi:10.1038/sj.leu.2404496; published online 21 December 2006
Keywords: hypercalcemia; childhood ALL; PTHrP; E2A-HLF; bisphosphonate

Introduction

Hypercalcemia is a frequent complication in adults with malignancy, and its incidence has been estimated as 5–20%.[1] In contrast, in the report from St Jude Children's Research Hospital, the incidence of hypercalcemia among children with malignancy who were treated from 1962 to 1991 was only 0.4%.[2] Among the 25 affected children reported from St Jude Children's Research Hospital, 10 had ALL including six cases of B-precursor ALL and three cases of mature B-ALL, and 14 had solid tumors including four cases of rhabdomyosarcoma. Therefore, hypercalcemia develops most commonly in ALL among childhood malignancies. Despite the importance in clinical management, owing to its relative rarity, the clinical characteristics of childhood ALL accompanied by hypercalcemia, mechanisms of hypercalcemia, response to current management for hypercalcemia and final outcome of ALL accompanied by hypercalcemia remain totally unclarified. There are two main mechanisms of hypercalcemia in malignancy: localized bone destruction by invasive cancer cells with the participation of various cytokines, and osteoclastic bone resorption mediated by humoral tumor-derived factors.[1,3,4] Hypercalcemia in malignancy is frequently mediated with parathyroid hormone-related peptide (PTHrP) by increasing osteoclastic bone resorption, renal resorption of calcium and renal phosphate loss.[5,6] Although several case reports showed the involvement of PTHrP in childhood ALL complicated with hypercalcemia,[7–9] its significance remains to be confirmed in a larger study.

t(17;19)(q21-q22;p13), which generates E2A-HLF fusion transcription factor,[10,11] is a rare translocation present in less than 1% of childhood ALL cases,[12] and its association with hypercalcemia, acquired coagulation abnormalities and extremely poor therapeutic outcome has been noticed.[13–16] The *E2A-HLF* fusion gene encodes a chimeric protein in which the transactivation domain of E2A links to the basic leucine zipper dimerization and DNA-binding domain of HLF.[10,11] E2A-HLF promotes anchorage-independent growth of murine fibroblasts[17,18] and protects cells from apoptosis owing to growth factor deprivation,[19–21] and *E2A-HLF* transgenic mice develop T-lineage lymphoid malignancies.[22,23] Although their significance in the clinical features has been controversial, there

Correspondence: Dr Takeshi Inukai, Department of Pediatrics, School of Medicine, University of Yamanashi, 1110 Shimokato, Chuo, Yamanashi 409-3898, Japan;
E-mail: tinukai@yamanashi.ac.jp
Received 28 September 2006; revised 19 October 2006; accepted 24 October 2006; published online 21 December 2006

are two types of fusion: type 1 is generated by the fusion between exon 13 of *E2A* and exon 4 of *HLF* with an insertion of cryptic exon (joining region) maintaining an open-reading frame, whereas type 2 is generated by the fusion between exon 12 of *E2A* and exon 4 of *HLF* in the same reading frame.[24] Of note, despite its rarity, two of the six B-precursor ALL patients with hypercalcemia reported from St Jude Children's Research Hospital showed t(17;19) on cytogenetic analysis,[2] and the two patients were confirmed to have *E2A-HLF* fusion.[10] Although these observations suggest the frequent association of t(17;19) with the development of hypercalcemia in childhood ALL, more detailed analyses of additional cases are needed to adequately address this point.

In this study, we undertook a retrospective review of 22 patients with childhood ALL other than mature B-ALL, who developed hypercalcemia at onset or relapse of ALL. We found that childhood ALL accompanied by hypercalcemia was frequently associated with t(17;19) and *E2A-HLF* expression, and that PTHrP-mediated hypercalcemia was revealed in the half of the 22 patients and over two-thirds of the patients in whom conclusive data were available.

Materials and methods

Patients and diagnosis criteria for PTHrP-mediated hypercalcemia

Hypercalcemia was defined as total serum calcium concentration of greater than 12.0 mg/dl. From 1990 to 2005, 25 patients with childhood ALL with L1 and L2 subtypes in French–American–British (FAB) classification developed hypercalcemia during their clinical course and were reported at medical meetings (Japan Pediatric Society, Japanese Society of Pediatric Hematology, The Japanese Society of Hematology, and Japanese Society of Clinical Hematology) or in medical journals in Japan, where approximately 500 children are estimated to develop ALL per year. Three patients were excluded from the analysis owing to either loss of medical record or lack of response from the responsible physician, and as a result, 22 patients were enrolled in this study. The diagnosis of PTHrP-mediated hypercalcemia was made by the following criteria: (1) positive immunohistochemistry of PTHrP in leukemia cells, (2) elevated serum C-terminal PTHrP (C-PTHrP) level accompanying a low serum level of intact PTH (iPTH) (<10 pg/ml) owing to a negative feedback loop, (3) elevated serum C-PTHrP level accompanied by normal serum creatinine level. As the serum level of C-PTHrP, but not intact PTHrP (iPTHrP), was reported to be nonspecifically high in renal insufficiency,[5] the diagnosis of PTHrP-mediated hypercalcemia was not concluded in the cases with elevated serum C-PTHrP level, in whom the serum creatinine level was elevated or not monitored and the iPTH level was not downregulated or not monitored. The upper limit of normal range for serum C-terminal PTHrP level varied from 40 to 61 pmol/l in each institute, and elevation of serum C-terminal PTHrP level was determined depending on each institutional normal range.

Reverse transcription (RT)-polymerase chain reaction (PCR) for E2A-HLF

RT-PCR analysis for *E2A-HLF* using patients' samples was approved by the institutional review board of the University of Yamanashi. Informed consent was obtained from the patients or the parents. Total RNA was isolated from bone marrow cells with Trizol (Life Technologies, Rockville, MD, USA) according to the manufacturer's instructions. RT was performed with 2 μg of total RNA, random hexamers and Superscript reverse transcriptase (Life Technologies) under conditions recommended by the manufacturer. PCR was performed using the following primers that were homologous to sequences in *E2A* exon 12 and exon 13, and *HLF* exon 4 (Figure 1a): *E2A* exon 12 (e12), 5′-gacatgcacacgctgctgcc-3′; E2A exon 13 (e13), 5′-gcctcatgcacaaccacgcg-3′; *HLF* exon 4 (e4), 5′-cccggatggcgatc tggttc-3′. Amplification was performed for 35 cycles at 94°C for 30 s, 56°C for 30 s and 72°C for 1 min. As a control, PCR for c-abl was performed under the same conditions using the following primers: *c-abl* sense, 5′-gtatcatctgactttgagcc-3′; *c-abl* antisense, 5′-gtaccaggagtgtttctcca-3′. The cell lines UOC-B1 and HAL-O1, which have type 1 fusion consisting of *E2A* exon 13 and *HLF* exon 4,[24] and Endo-kun, which has type 2 fusion consisting of *E2A* exon 12 and *HLF* exon 4[24] and was established from case 1, were used as positive controls.

Statistical analysis

All statistical analyses were performed with StatView (version 5.0.1) software. Event-free survival (EFS) was estimated according to Kaplan–Meier analysis. The starting point was the date of diagnosis of ALL, and the end point was relapse. Time was censored at last follow-up, and follow-up was updated in February 2006. Univariate comparison of EFS in different groups of patients was performed using the log-rank test, and χ^2-test and Student's *t*-test were used to assess the association between different characteristics.

Results

Characteristics of leukemia

The main clinical features of the 22 patients with ALL who developed hypercalcemia are summarized in Table 1. Although observation period was not completely identical, their clinical features were compared with those of the childhood ALL patients in the Tokyo Children's Cancer Study Group (TCCSG) treated with L89-12 (1989–1992, 418 patients) and L92-13 (1992–1995, 347 patients) protocols (Table 2),[25] in which approximately 20% of the patients in Japan were registered and Cases 3, 5 and 9 were enrolled. The incidence of age greater than 10 years at diagnosis of ALL in the present study (50%) was significantly higher ($P=0.005$) than that in the childhood ALL cases reported from TCCSG (23.8%). The male–female ratio was 54.5% and was identical to that in the childhood ALL cases reported from TCCSG (54.6%). Initial white blood cell count (WBC) of the cases with hypercalcemia ranged from 2 to 90×10^9/l (median, 6.2×10^9/l) and leukemic blasts were undetectable in the peripheral blood in eight patients. The rate of WBC $< 20 \times 10^9$/l (90.9%) was significantly higher ($P=0.010$) than the respective rate in childhood ALL reported from TCCSG (64.6%). The rates of severe anemia (hemoglobin < 8 g/dl) (27.3%) and thrombocytopenia (platelet count $< 100 \times 10^9$/l) (36.4%) were significantly lower ($P=0.025$ and 0.004, respectively) than those in childhood ALL in the TCCSG (51.1 and 66.1%, respectively). Intravenous coagulopathy was noticed in five of 20 patients. All of the patients except for Case 20 with dry tap marrow showed B-precursor immunophenotype. No patient showed T-cell immunophenotype. The incidence of T-cell immunophenotype (0%) tended to be low ($P=0.098$) compared with that in childhood ALL reported from the TCCSG (11.6%). Negative to low expression of CD19 (< 30%) was noted in two patients (Cases 19 and 21), and expression of CD13 and CD33

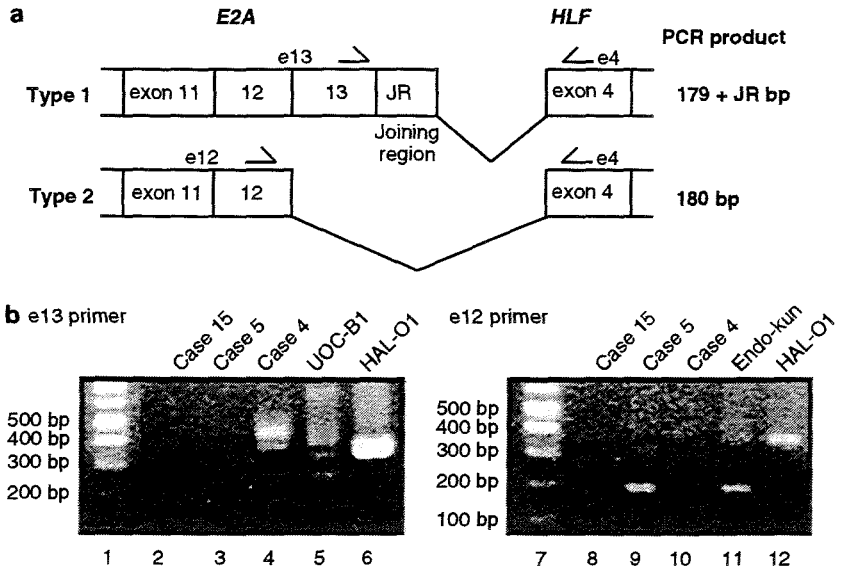

Figure 1 Representative analysis of RT-PCR amplification of *E2A-HLF*. (**a**) Schematic representation of two types of fusion. Type 1 is generated by fusion between exon 13 of *E2A* and exon 4 of *HLF* with an insertion of cryptic exon (joining region; JR) maintaining an open reading frame, whereas type 2 is generated by fusion between exon 12 of *E2A* and exon 4 of *HLF* in the same reading frame. The relative positions of the primers used to amplify the two types of *E2A-HLF* fusion complementary DNAs are shown. PCR using e13 and e4 primers is expected to generate a 179-bp + JR product from type 1 fusion but no product from type 2 fusion, whereas PCR using e12 and e4 primers generates a 180-bp product from type 2 fusion and 303-bp + JR product from type 1 fusion. (**b**) RT-PCR of *E2A-HLF* fusion. The left panel indicates the PCR products using e13 and e4 primers, and the right panel indicates the PCR products using e12 and e4 primers. Type 1 *E2A-HLF* was confirmed in Case 4 (lanes 4 and 10) as UOC-B1 (lane 5) and HAL-01 (lane 6), and type 2 *E2A-HLF* was confirmed in Case 5 (lanes 3 and 9) as Endo-kun (lane 11). None of the *E2A-HLF* transcripts was detectable in Case 15 (lanes 2 and 8). Lanes 1 and 7 demonstrate the molecular size marker. The RT-PCR product of *c-abl* was confirmed in each of the samples (data not shown).

($\geqslant$10%) was confirmed in 6 (Cases 1, 2, 5, 6, 10 and 22) and eight patients (Cases 1, 2, 3, 4, 5, 9, 18 and 22), respectively.

Incidence of t(17;19)

On karyotypic analysis (Table 1), metaphase was not obtained in five patients, and normal karyotype was revealed in nine patients. Cases 1 and 4 harbored t(17;19)(q21;p13) and add(19)(p13) at disease onset, respectively. Cases 2, 3 and 5 who showed normal karyotype at onset, harbored t(17;19)(q21;p13) at relapse. RT-PCR analysis of *E2A-HLF* was performed in nine patients in whom frozen marrow samples were available (Table 1 and Figure 1). Type 1 *E2A-HLF* was detected in Cases 2 and 4, whereas type 2 *E2A-HLF* was detected in Cases 1, 3 and 5. In contrast, *E2A-HLF* transcripts were not detectable in Cases 7, 8, 15 and 18, who showed neither add(19)(p13) nor t(17;19)(q21;p13) in the cytogenetic study. Of note, all five patients with t(17;19)-ALL expressed CD33 (Table 1) and the incidence of CD33 expression among patients with t(17;19)-ALL was significantly higher than that among the other 16 patients ($P=0.002$ by χ^2-test). Three patients with t(17;19)-ALL had L2 phenotype (Table 1) and the incidence of L2 phenotype among patients with t(17;19)-ALL was significantly higher than that among the other patients ($P=0.008$ by χ^2-test). Four patients with t(17;19)-ALL developed the disease at age greater than 10 years, and two patients had coagulopathy.

Clinical characteristics of hypercalcemia

Hypercalcemia was present at the time of original diagnosis in 18 patients and at disease recurrence in four patients (Cases 1, 2, 5 and 7), and a diagnosis of hypercalcemia was made before treatment. Table 3 summarizes the clinical symptoms and laboratory data at diagnosis except for serum levels of blood–urea–nitrogen and creatinine, which were shown as the highest values before resolution of hypercalcemia. The total serum calcium concentration was 15 mg/dl or greater in 16 patients (72.7%). At least one clinical symptom associated with hypercalcemia was observed in all patients and the incidence of each symptom was as follows: emesis in 11 patients (50%), bone pain in 13 patients (59.1%), osteolytic lesion in 14 patients (63.6%), fracture of the vertebral bone in four patients (18.2%), and renal insufficiency with elevated serum creatinine level to 1.0 mg/dl or higher in 14 (66.7%) of 21 patients. Elevated serum creatinine was associated with older children ($\geqslant$10 years old) ($P=0.0002$ by χ^2-test) and infrequently associated with hypophosphatemia ($\leqslant$4 mg/dl) ($P=0.02$ by χ^2-test).

Mechanisms of the development of hypercalcemia

The serum C-terminal PTHrP (C-PTHrP) level was elevated in 15 of the 16 patients assayed (Table 3). The diagnosis of PTHrP-mediated hypercalcemia was made by positive immunohistochemistry of PTHrP in leukemia cells in the two patients assayed (Cases 6 and 7). The seven patients with an elevated serum C-PTHrP level (Cases 1, 2, 3, 8, 9, 10 and 11) accompanying a low serum level of iPTH owing to a negative feedback loop were diagnosed to have typical PTHrP-mediated hypercalcemia. Cases 12 and 13 with elevated serum C-PTHrP level accompanied by normal serum creatinine level were concluded to have PTHrP-mediated hypercalcemia. In contrast, Cases 4, 14, 15, 16 and 17 with elevated serum C-PTHrP level, in whom the serum creatinine level was elevated or missing and the iPTH

Table 1 Clinical and laboratory characteristics of the patients with ALL with hypercalcemia

	Age/sex (year)	Initial WBC ($\times 10^9$/l)	Blast (%)	Hb (g/dl)	Plt ($\times 10^9$/l)	FAB	Coagulopathy	Cell surface antigen CD (%)				Cytogenetics	E2A-HLF mRNA	EFS(m)	Relapse	Ref.
								10	19	13	33					
t(17;19) positive																
1	14/F	24.1	63	8.4	51	L2	–	85	90	22	32	46,XX,t(17;19)(q21;p13)	Type 2	9	+	16
2	10/M	3.2	4	8.1	127	L2	+	92	92	79	60	46,XY,t(17;19)(q21;p13)[a]	Type 1	14	+	
3	4/M	7.3	4	7.3	144	L1	–	81	87	2	10	46,XY,t(17;19)(q21;p13)[a]	Type 2	5	+	15
4	14/F	4.2	0	8.7	128	L1	–	97	98	8	86	46,XX,13,del(13)(q14q22),add(19)(p13)	Type 1	3	+	9
5	12/F	90.0	88	8.4	32	L2	+	63	72	13	62	51,XX, +8,t(17;19),(q21;p13), +18,+21,+21,+22[a]	Type 2	2	+	16
t(17;19) negative or not confirmed																
6	14/M	4.9	12	12.0	164	L1	–	93	92	10	1	No metaphase	NA	+49	–	
7	12/M	13.1	52	11.8	23	L2	–	29	63	NT	4	46,XY, −21,+13,-9, t(8;9)(q13;p22)	Neg.	8	+	7
8	8/F	19.8	7	11.1	142	L1	–	60	92	0	1	46,XX,t(15;17)(q13;q21)	Neg.	+154	–	
9	10/F	5.1	0	10.7	138	NA	–	8	96	2	6	46,XY	NA	+51	–	
10	10/M	5.7	0	12.2	176	L1	+	91	100	60	18	No metaphase	NA	+66	–	
11	10/M	4.7	2	8.0	92	L1	+	58	69	4	2	46,XY	NA	32	+	
12	2/F	10.0	12	6.9	206	L1	–	55	NT	1	NT	46,XX	NA	+236	–	8
13	8/M	5.2	0	9.1	324	L1	NA	60	54	2	4	46,XY	NA	58	+	8
14	11/M	6.6	19	14.2	193	L1	–	37	95	5	3	46,XY	NA	19	+[b]	
15	5/M	8.9	26	7.3	76	L1	+	50	100	1	1	No metaphase	Neg.	+35	–	
16	7/F	6.2	40	9.4	30	L1	–	55	99	1	0	46,XX	NA	+147	–	8
17	3/F	12.1	0	9.1	399	L1	NA	35	68	8	5	46,XX	NA	+49	–	8
18	10/M	12.7	28	11.2	248	L1	–	35	37	5	14	44,add(X)(q22),del(Y)(q12),−4,−8,−9,+mar	Neg.	11	+	
19	2/M	5.9	0	7.1	184	L1	–	98	3	5	3	46,XY	NA	35	+	30
20	6/F	3.3	0	5.9	55	L1	–		NT(dry tap)			NT(dry tap)	NA	+127	–	
21	2/F	14.8	0	11.0	200	L1	–	89	25	4	4	46,XX	NA	+19	–	30
22	7/F	2.0	3	5.9	54	L1	–	97	96	74	33	No metaphase	NA	+83	–	

Abbreviations: ALL, acute lymphoblastic leukemia; EFS, event-free survival; F, female; FAB, French–American–British; Hb, hemoglobin; M, male; m, month; Ref, reference; NA, data or samples not available; NT, not tested; Neg, negative; Plt, platelet count.
[a]Karyotype at relapse is indicated, but normal karyotype was obtained at diagnosis.
[b]Relapsed as AML.

level was not downregulated or missing, were not concluded to have PTHrP-mediated hypercalcemia. iPTHrP was undetectable in serum in all four patients assayed (Cases 18, 19, 20 and 21), indicating that the involvement of PTHrP in their hypercalcemia is excluded. Among these four patients, the serum phosphorus level was low and serum 1,25-$(OH)_2$ vitamin D (calcitriol) level was normal in the three patients assayed, indicating that involvement of calcitriol-mediated hypercalcemia is unlikely because it is characterized by elevated calcitriol level accompanied by normal serum phosphorus level.[4] In Case 22, iPTH was markedly elevated but C-PTHrP was normal in the serum, suggesting ectopic production of PTH by leukemia cells. Collectively, among the 21 patients whose PTHrP data were available, involvement of PTHrP-mediated hypercalcemia was confirmed in 11 patients (Cases 1, 2, 3, 6, 7, 8, 9, 10, 11, 12 and 13) but ruled out in five patients (Cases 18, 19, 20, 21 and 22). Of importance, hypercalcemia was definitely mediated by PTHrP in all three patients with t(17;19)-ALL in whom informative data were available (Cases 1, 2 and 3).

Table 2 Comparison of characteristics of patients in present study and patients with childhood ALL in the TCCSG

	Present study		*TCCSG*[a]		χ^2-*test*
	Incidence	*%*	*Incidence*	*%*	*P-value*
Age ⩾10 years	11/22	50.0	182/765	23.8	$P=0.005$
Male	12/22	54.5	418/765	54.6	$P=0.993$
WBC $<20\times10^9$/l	20/22	90.9	490/764	64.6	$P=0.010$
Hb <8 g/dl	6/22	27.3	387/757	51.1	$P=0.025$
Plt $<100\times10^9$/l	8/22	36.4	501/758	66.1	$P=0.004$
T-ALL	0/21	0.0	84/725	11.6	$P=0.098$

Abbreviations: ALL, acute lymphoblastic leukemia; Hb, hemoglobin; Plt, platelet count; TCCSG, Tokyo Children's Cancer Study Group; WBC, white blood cell count.
[a]The data of 765 childhood ALL patients excluding B-ALL and infants in the L89-12 and L92-13 study.

Management of hypercalcemia

Intravenous hydration with or without furosemide was administered to all patients. In Case 5, the hypercalcemia resolved without additional therapy. Fifteen patients received calcitonin (Cases 1, 2, 3, 4, 6, 7, 9, 10, 12, 13, 14, 16, 17, 18 and 22), 11 patients received bisphosphonate (Cases 2, 4, 6, 9, 10, 11, 15, 18, 19, 21 and 22), and seven of those patients received both calcitonin and bisphosphonate. Ten of the 12 patients who were diagnosed in or after 1997 received bisphosphonate, whereas only one of the 10 patients diagnosed before 1997 did so. Among the 17 patients who received chemotherapy before resolution of hypercalcemia (Cases 1, 2, 3, 7, 8, 9, 10, 11, 12, 13, 14, 16, 17, 18, 19, 20 and 22), chemotherapy was started by oral predonisolone (PSL) alone in seven patients (Cases 2, 9, 10, 11, 18, 19 and 22). Hypercalcemia and renal insufficiency ultimately resolved in all patients treated with or without bisphosphonate (Figure 2). As summarized in Table 4, although the levels of serum calcium before treatment and the incidences of concomitant use of chemotherapy and calcitonin were equivalent between the patients treated with and without bisphosphonate, rapid reduction of serum calcium level (<10 mg/dl within 4 days) was observed significantly more often in patients who were treated with bisphosphonate than in patients who were not treated with bisphosphonate. Consistently, the serum creatinine level tended to decrease

Table 3 Clinical and laboratory characteristics of hypercalcemia complicated in the patients with ALL

Case	*Ca (mg/dl)*	*Pi (mg/dl)*	*PTHrP (pmol/l)*		*iPTH (pg/ml)*	*1,25 $(OH)_2D$ (pg/ml)*	*BUN (mg/dl)*	*Cr (mg/dl)*	*Bone Pain*	*Osteolytic lesion*	*Emesis*
			C	*Intact*							
t(17;19) positive											
1	15.7	5.4	72		<1	NT	81	2.9	+	+	−
2	16.5	5.7	124		<3	<5	39	1.9	−	−	+
3	12.7	3.3	110		<3	NT	31	0.6	+	−	−
4	16.6	4.0	92		15.0	NT	28	2.6	+	+	−
5	12.9	2.6		NT	7.0	NT	76	3.4	−	−	−
t(17;19) negative or not confirmed											
6	16.3	4.9	76[a]		NT	5.5	49	2.3	+	−	−
7	14.6	4.2		NT[a]	<5	NT	44	1.45	+	+	+
8	19.2	3.9	107		7.0	26.0	36	0.9	−	+	−
9	20.0	5.0	114		<10	NT	62	1.2	−	−	+
10	14.3	4.6	46		9.0	2.8	34	1.8	+	+[b]	−
11	12.2	6.2	57		<1	<10	52	2.4	+	+[b]	+
12	20.8	3.2	240		NT	NT	39	0.6	−	+	+
13	15.0	4.5	75		NT	<5	19	0.6	+	+[b]	+
14	15.0	5.0	108		18.3	NT	58	2.4	−	+	+
15	15.0	4.5	134		NT	NT	33	1.6	−	−	−
16	15.8	4.9	112		NT	14.3	55	1.4	−	+	+
17	14.6	NA	100		NT	14.0	NA	NA	+	+	−
18	17.4	2.7		<1.1	12.7	3.8	24	1.3	+	+[b]	+
19	15.8	3.6		<1.1	7.0	8.0	8	0.3	+	+	−
20	15.4	2.8		<1.1	13.4	NT	16	0.6	+	−	−
21	16.6	3.5		<1.1	4.2	12.0	15	0.3	+	+	+
22	19.1	7.6	<1		86.0	NT	NA	0.9	−	−	+

Abbreviations: ALL, acute lymphoblastic leukemia; BUN, blood–urea–nitrogen; C, C-terminal; Cr, creatinine; iPTH, intact PTH; NA, data or sample not available; NT, not tested; PTHrP, parathyroid hormone-related peptide.
[a]Positive for immunohistochemistry of PTHrP in leukemia cells.
[b]Fracture of the vertebral bone was disclosed by X-ray.

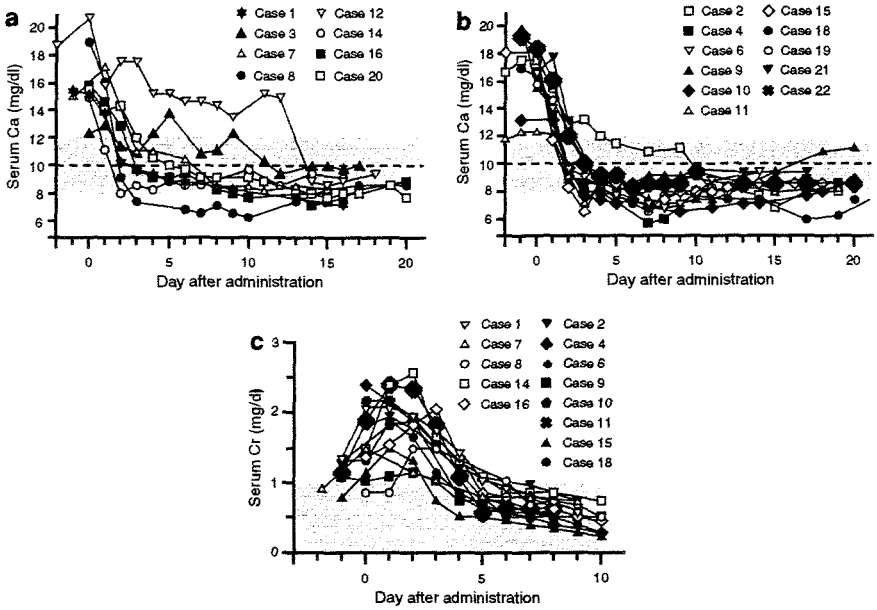

Figure 2 Changes in serum calcium (Ca) and creatinine (Cr) levels. Changes in the serum Ca level of the eight patients who were not treated with bisphosphonate (**a**) and the 11 patients who were treated with bisphosphonate (**b**) and changes in the serum Cr level of the patients who were (closed symbols) or were not (open symbols) treated with bisphosphonate, whose maximum level of serum Cr exceeded 1 mg/dl (**c**). The day of administration of the first dose of bisphosphonate was defined as day 0.

Table 4 Comparison of clinical course of hypercalcemia between patients who were or were not treated with bisphosphonate

	Bisphosphonate (n = 11)	*Others (n = 8)*	*P-value (t-test/χ^2-test)*
Serum Ca level			
Pre-therapy	16.0±0.6 mg/dl	16.0±1.0 mg/dl	$P=0.973^a$
Maximum	16.8±0.7 mg/dl	16.4±0.9 mg/dl	$P=0.708^a$
Minimum	6.8±0.2 mg/dl	7.7±0.3 mg/dl	$P=0.024^a$
Chemotherapy			
Started	8	7	$P=0.436$
Not started	3	1	
Calcitonin			
Administered	7	6	$P=0.599$
Not administered	4	2	
Ca <12 mg/dl on day 2			
Yes	7	3	$P=0.260$
No	4	5	
Ca <10 mg/dl on day 4			
Yes	10	4	$P=0.046$
No	1	4	
Minimum Ca <8 mg/dl			
Yes	9	3	$P=0.048$
No	2	5	
Ca supplementation			
Yes	5	0	$P=0.026$
No	6	8	
Cr <1 mg/dl on day 5			
Yes	7	2	$P=0.071$
No	1	3	

Abbreviations: Ca, serum calcium level; Cr, serum creatinine level.
[a]The *P*-value was analyzed by *t*-test.

more rapidly in patients who were treated with bisphosphonate compared with those who were not treated with bisphosphonate. The minimum serum calcium level of the patients treated with bisphosphonate was significantly lower than that of the patients treated without bisphosphonate, and hypocalcemia (<8 mg/dl) developed more frequently in the